JNeurosci
THE JOURNAL OF NEUROSCIENCE

Research Articles: Cellular/Molecular

Demethylation of G protein-coupled receptor 151 promoter facilitates the binding of Kruppel-like factor 5 and enhances neuropathic pain after nerve injury in mice

Bao-Chun Jiang[1], Wen- Wen Zhang[1], Tian Yang[1], Chang-Yun Guo[1], De-Li Cao[1], Zhi-Jun Zhang[1,2] and Yong-Jing Gao[1,3]

[1]*Pain Research Laboratory, Institute of Nautical Medicine, Nantong University, Jiangsu 226019, China*
[2]*Department of Human Anatomy, School of Medicine, Nantong University, Jiangsu 226001, China*
[3]*Co-innovation Center of Neuroregeneration, Nantong University, Jiangsu 226001, China*

https://doi.org/10.1523/JNEUROSCI.0702-18.2018

Received: 15 March 2018

Revised: 13 September 2018

Accepted: 22 October 2018

Published: 29 October 2018

Author contributions: B.-C.J., W.-W.Z., T.Y., C.-Y.G., D.-L.C., and Z.-J.Z. performed research; B.-C.J., W.-W.Z., T.Y., and Y.-J.G. analyzed data; B.-C.J. wrote the first draft of the paper; Y.-J.G. designed research; Y.-J.G. edited the paper; Y.-J.G. wrote the paper.

Conflict of Interest: The authors declare no competing financial interests.

We thank Prof. Yu-Qiang Ding for providing GAD67-GFP+ mice. This study was supported by the grants from the National Natural Science Foundation of China (NSFC 81400915, 81771197, 31671091, 81571070, 31700899, and 31871064), the Natural Science Foundation of Jiangsu Province (BK20171255, BK20140427). The authors declare no competing financial interests.

Correspondence: Yong-Jing Gao, Institute of Nautical Medicine, Nantong University, 9 Seyuan Road, Nantong, Jiangsu 226019, China. Tel: +86-513-55003374; Fax: +86-513-55003370; Email: gaoyongjing@hotmail.com or gaoyongjing@ntu.edu.cn

Cite as: J. Neurosci 2018; 10.1523/JNEUROSCI.0702-18.2018

Demethylation of G protein-coupled receptor 151 promoter facilitates the binding of Kruppel-like factor 5 and enhances neuropathic pain after nerve injury in mice

Bao-Chun Jiang,[1#] Wen-Wen Zhang,[1#] Tian Yang,[1#] Chang-Yun Guo,[1] De-Li Cao,[1] Zhi-Jun Zhang,[1,2] Yong-Jing Gao[1,3*]

1. Pain Research Laboratory, Institute of Nautical Medicine, Nantong University, Jiangsu 226019, China
2. Department of Human Anatomy, School of Medicine, Nantong University, Jiangsu 226001, China
3. Co-innovation Center of Neuroregeneration, Nantong University, Jiangsu 226001, China

Running title: Demethylation of GPR151and neuropathic pain

Number of words in Abstract: 245; Introduction: 649; Discussion: 1500

Number of figures: 9

Number of tables: 3

# These authors contributed equally to this work.

*** Correspondence:**

Yong-Jing Gao, Institute of Nautical Medicine, Nantong University, 9 Seyuan Road, Nantong, Jiangsu 226019, China.

Tel: +86-513-55003374; Fax: +86-513-55003370;

Email: gaoyongjing@hotmail.com or gaoyongjing@ntu.edu.cn

Acknowledgements

We thank Prof. Yu-Qiang Ding for providing GAD67-GFP^{+} mice. This study was supported by the grants from the National Natural Science Foundation of China (NSFC 81400915, 81771197, 31671091, 81571070, 31700899, and 31871064), the Natural Science Foundation of Jiangsu Province (BK20171255, BK20140427). The authors declare no competing financial interests.

Abstract

G protein-coupled receptors are considered to be cell surface sensors of extracellular signals, thereby having a crucial role in signal transduction and being the most fruitful targets for drug discovery. G protein-coupled receptor 151 (GPR151) was reported to be expressed specifically in the habenular area. Here we report the expression and the epigenetic regulation of GRP151 in the spinal cord after spinal nerve ligation (SNL) and the contribution of GPR151 to neuropathic pain in male mice. SNL dramatically increased GPR151 expression in spinal neurons. *GPR151* mutation or spinal inhibition by shRNA alleviated SNL-induced mechanical allodynia and heat hyperalgesia. Interestingly, the CpG island in the *GPR151* gene promoter region was demethylated, the expression of DNA methyltransferase 3b (DNMT3b) was decreased, and the binding of DNMT3b with *GPR151* promoter was reduced after SNL. Overexpression of DNMT3b in the spinal cord decreased *GPR151* expression and attenuated SNL-induced neuropathic pain. Furthermore, Kruppel-like factor 5 (KLF5), a transcriptional factor of the KLF family, was upregulated in spinal neurons, and the binding affinity of KLF5 with *GPR151* promoter was increased after SNL. Inhibition of KLF5 reduced *GPR151* expression and attenuated SNL-induced pain hypersensitivity. Further mRNA microarray analysis revealed that mutation of *GPR151* reduced the expression of a variety of pain-related genes in response to SNL, especially mitogen-activated protein kinases (MAPKs) signaling pathway-associated genes. This study reveals that GPR151, increased by DNA demethylation and the enhanced interaction with KLF5, contributes to the maintenance of neuropathic pain via increasing MAPKs pathway-related gene expression.

Significance statement

G protein-coupled receptors (GPCRs) are targets of various clinically approved drugs. Here we report that SNL increased GPR151 expression in the spinal cord, and mutation or inhibition of GPR151 alleviated SNL-induced neuropathic pain. In addition, SNL downregulated the expression of DNMT3b, which caused demethylation of *GPR151* gene promoter, facilitated the binding of transcriptional factor KLF5 with the *GPR151* promoter, and further increased GPR151 expression in spinal neurons. The increased GPR151 may contribute to the pathogenesis of neuropathic pain via activating MAPKs signaling and increasing pain-related genes expression. Our study reveals an epigenetic mechanism underlying GPR151 expression and suggests that targeting GPR151 may offer a new strategy for the treatment of neuropathic pain.

89 **Introduction**

90 G protein-coupled receptors (GPCRs) are a superfamily of cell-surface receptors that sense
91 various extracellular signals including neurotransmitters, hormones, and growth factors, and
92 ultimately resulting in the activation of intracellular signaling pathways (Hauser et al., 2017). Of
93 the druggable molecules in the human genome, GPCRs are the targets of approximately 40% of
94 clinically approved drugs (Wolf, 2013). Orphan GPCRs (oGPCRs) are a group of GPCRs whose
95 endogenous ligands have not yet been identified. Unraveling the biological functions of oGPCRs
96 will help to understand the physiological and pathological processes and to identify new potential
97 drug targets.

98 GPR151 is one of oGPCRs, with its gene map to chromosome 5q32 in human and to 18B3 in
99 mice. The functions of GPR151 are mostly unknown as no endogenous or synthetic ligand for this
100 receptor has been reported yet. GPR151 was originally identified as galanin receptor based on its
101 amino acid sequence similarity with galanin receptors 2 and 3, but responds only very weakly to
102 the neuropeptide galanin (Ignatov et al., 2004). Previous studies demonstrated that GPR151 is
103 highly enriched in rodent medial and lateral habenula (Kobayashi et al., 2013; Broms et al., 2015)
104 where it extensively projects to the interpeduncular nucleus, the rostromedial tegmental area, the
105 rhabdoid nucleus, and the mesencephalic raphe nuclei (Broms et al., 2015). Moreover, the fibers
106 overlap with cholinergic, substance P-ergic and glutamatergic markers (Broms et al., 2015). These
107 findings suggest that GPR151 may be involved in habenula–related functions, such as depression,
108 negative reward, decision-making, nicotine withdrawal, and pain (Broms et al., 2017). However,
109 the expression and the role of GPR151 in other areas of the CNS remain largely unknown.

110 Peripheral sensitization in the dorsal root ganglion (DRG) and central sensitization in the

spinal cord play an important role in the pathogenesis of neuropathic pain (Hehn et al., 2012). Recent studies using mRNA microarray analysis showed that *GPR151* mRNA was highly upregulated in the DRG after chronic constriction injury (CCI)-induced neuropathic pain (Reinhold et al., 2015) or burn injury-induced pain (Yin et al., 2016). *GPR151* was also dramatically increased in the spinal cord after spinal nerve ligation (SNL)-induced neuropathic pain in mice (Jiang et al., 2015). These studies indicate that GPR151 in the DRG and spinal cord may be involved in neuropathic pain. However, Holmes et al. recently reported that deletion of *GPR151* did not affect acute pain, inflammatory pain and neuropathic pain behaviors (Holmes et al., 2016).

Several lines of evidence indicate that gene expression is regulated by epigenetic mechanisms (Niederberger et al., 2017). DNA methylation is a main epigenetic mechanism that modulates the compact of chromatin and the repression of gene expression (Cedar and Bergman, 2012). DNA methyltransferases (DNMTs) are important in regulating DNA methylation and directly inhibit transcription by interfering with transcription factor binding (Lyko, 2017). Kruppel-like factors (KLFs) are a 17-member family of zinc finger-containing transcription factors (Moore et al., 2009). KLF7 is required for the development of a subset of nociceptive sensory neurons by specifically regulating TrkA gene expression (Lei et al., 2005). Specific inhibition of KLF6, KLF9, and KLF15 by intrathecal DNA decoys alleviated mechanical hypersensitivity in the spared nerve injury (SNI)- or CCI-induced neuropathic pain in rats (Mamet et al., 2017a). The promoter region of the *GPR151* gene contains 5 consensus binding motifs of KLF5. Whether *GPR151* expression is regulated by DNA methylation and KLF5 under neuropathic pain condition has not been investigated.

In the present work, we provide evidence that SNL increased GPR151 expression in the spinal neurons, and mutation or knockdown of *GPR151* alleviated SNL-induced neuropathic pain. Our results also demonstrate that *GPR151* expression is regulated by DNMT3b-mediated DNA demethylation and KLF5-mediated increase of transcription. The mRNA microarray analysis further revealed that GPR151 might regulate neuropathic pain via the activation of mitogen-activated protein kinases (MAPKs) signaling pathway, which has been demonstrated to play a vital role in the pathogenesis of chronic pain (Ji et al., 2009; Anand et al., 2011).

Materials and methods

Animals and surgery

Adult ICR mice and C57BL/6 (male, 6-8 weeks, RRID: MGI: 5656552) mice were purchased from the Experimental Animal Center of Nantong University. *GPR151*$^{-/-}$ mice were generated by Cyagen (Cyagen Biosciences Inc, China). The animals were maintained in SPF facilities on a 12:12 light-dark cycle at a room temperature of 22 ± 1℃ with free access to food and water. The experimental procedures were approved by the Animal Care and Use Committee of Nantong University and performed in accordance with guidelines of the International Association for the Study of Pain. To produce SNL, animals were anesthetized with isoflurane, and the L6 transverse process was removed to expose the L4 and L5 spinal nerve. The L5 spinal nerve was then isolated and tightly ligated with 6-0 silk thread (Jiang et al., 2016). For sham-operated mice, the L5 spinal nerve was exposed but not ligated.

Generation of TALEN-mediated *GPR151* mutant mice

155 Transcription activator-like (TAL) effector nucleases (TALENs) were used to create *GPR151*
156 mutant mice (GenBank accession number of *GPR151*: NM-181543.1). TALENs were designed to
157 target exon 1 of *GPR151* using the TALENdesigner software (TALEs-L: 5'-TGG AGG ACC ATC
158 ATT CCG-3'; Spacer: 5'-TCT CTC TTG ATG GCC GTG TGC-3'; TALEs-R: 5'-TCC CAC GAG
159 ACC CAC CAG-3'. Fig. 1A). TALEN mRNAs were generated by in vitro transcription and
160 injected into fertilized eggs of C57BL/6. The binding of TALENs with the GPR151 genome loci
161 induced a site-specific double-strand break (DSB) followed by non-homologous end joining
162 (NHEJ) repair, resulting in the deletion of some bases (Fig. 1A). The chimera mice were identified
163 by DNA sequencing (primer: 5′-GCC GAC ACC AAT TCC AGC AAC-3′. Fig. 1B).
164

165 **DNA extraction and genotyping**

166 About 3 mm of the mouse tails were cut, and DNA was extracted with the phenol-chloroform
167 method. PCR was performed to identify WT or *GPR151* mutant mice. The following primers were
168 used (forward: 5'-TCC AAG GAC TGG AGG ACC AT-3', reverse: 5'-CAC ACA GGT TTC CCA
169 CGA GA-3'. WT: 76 bp, *GPR151*$^{-/-}$: 69 bp). For PCR amplification, approximately 500 ng DNA
170 was used in a 50 μl reaction volume containing 25 μl 2× Taq PCR MasterMix (Tiangen Biotech)
171 and 1 μM primers. Reactions initially were denatured at 94°C for 3 minutes followed by 35 cycles
172 at 94°C for 30 seconds, 60°C for 30 seconds, 72°C for 30 seconds and a final extension at 72°C
173 for 2 minutes. Amplicons were separated using 3% agarose gel, stained with DuRed (Biotium) and
174 photographed with GelDoc-It Imaging System (UVP).
175

176 **Drugs and administration**

5′-cholesteryl and 2′-O-methyl-modified small interfering RNA (siRNA) for *DNMT3b* or *KLF5*, and an additional scrambled siRNA were purchased from RiboBio Inc (Guangzhou, China). A potent KLF5 inhibitor, ML264 was purchased from Selleckchem (Houston, USA). Intrathecal injection (i.t.) was made with a 30-G needle between the L5 and L6 level to deliver the reagents to the cerebral spinal fluid.

Real-time PCR

The total RNA of L5 spinal cord was extracted using TRIzol reagent (Invitrogen, Life Technologies). One microgram total RNA was converted into cDNA through Prime ScriptTM RT reagent Kit (TaKaRa, Japan). PCR reactions were performed on a Light Cycler 96 RT-PCR system (Roche Diagnostics) using FastStart Essential DNA Green Master (Roche Diagnostics) for detecting. The primer sequences for each gene are listed in Table 1. The PCR amplifications were performed at 95 °C for 600 s, followed by 45 cycles of thermal cycling at 95 °C for 10 s, 60 °C for 10 s and 72°C for 10 s. *GAPDH* was used as endogenous control to normalize differences. The data was analyzed through LightCycler96 software and evaluated using the Comparative CT method ($2^{-\Delta\Delta CT}$).

Single-cell PCR

All the facilities used for single-cell PCR experiment were treated with DEPC before use. The reagents were prepared according to the instruction to remove the genomic DNA (Invitrogen). The single cell was collected in the mixture using glass electrode from the acute isolation of L5 spinal dorsal horn sections. The first step of reverse transcription system was performed at 37℃ for 40

min and then at 80℃ for 10 min to stop the reaction. As for the second step for reverse transcription (Invitrogen), the collections were performed at 50℃ for 50 min and 70℃ for 15 min to stop the reaction. The harvested cDNA fragments were then amplified using the constructed *GPR151*, *NeuN* and *GAPDH* outer primers (Table 2) for 30-40 cycles at 58℃ for 10 s and at 72℃ for 30 s. The PCR productions were diluted for 1000 folds to be further amplified using constructed inner primers (Table 2) for 30 cycles at 58℃ for 10 s and 72℃ for 30 s. The final PCR products were visualized by GelRed (Biotium) staining in 3% agarose gels.

Methylation-specific PCR (MSP)

The genomic DNA was extracted through a QIAamp DNA Mini Kit (Qiagen, Hilden, Germany) according to the manufacturer's protocol. Sodium bisulfite conversion of genomic DNA was performed using an EpiTect Bisulfite Kit (Qiagen, Germany). Bisulfite-converted genomic DNA was amplified with EpiTect Master Mix for MSP (Qiagen) with methylation-specific or unmethylation-specific primers (Table 3). The PCR products were analyzed by electrophoresis. The percentage of methylation of the *GPR151* promoter from the spinal cord of SNL- or sham-operated animals was detected through densitometric analysis of MSP products (ratio of methylated products to unmethylated products).

Bisulfite Sequencing PCR (BSP)

The genomic DNA extraction and bisulfite treatment were performed as described in the MSP method. PCR was performed to amplify the CpG island fragment of the *GPR151* promoter from bisulfite-converted genomic DNA using the primers shown in Table 3. Then the PCR products

221 were purified with the QIAquick Gel Extraction Kit (Qiagen). The eluted DNA fragments were
222 ligated into pGEM-T Easy Vector (Promega Corporation, USA) for sequencing. Ten colonies for
223 each mouse were randomly chosen for sequencing.
224
225 ***GPR151* promoter activity analysis**
226 The *GPR151* promoter reporter cloned into the pCpG-free basic reporter vector (InvivoGen) was
227 either methylated by incubation with S-adenosyl methionine or unmethylated in the presence or
228 absence of CpG methylase M.SssI (Fisher Thermo Scientific). The methylated or unmethylated
229 pCpG-free-*GPR151*-Lucia luciferase reporter plasmid was transfected into HEK293 cells (CLS,
230 catalog #300192/p777_HEK293, RRID: CVCL_0045) by Lipofectamine 3000 (Invitrogen).
231 Meanwhile, the cells were cotransfected with *KLF5* overexpression plasmid. The activity of
232 secreted coelenterazine luciferase in the medium was detected 48 h later using the Dual-Luciferase
233 Assay System (Promega) following the instructions. Twenty microliters of the medium samples
234 were subjected to luciferase assay (Synergy 2 Multi-Mode Reader, BioTEL). The predicted five
235 mutant KLF5 binding sites (BS1-5) in *GPR151* gene promoter of luciferase reporter vectors were
236 purchased from Sangon Biotech and were cotransfected with *KLF5* overexpression plasmid in
237 HEK-293 cells. The activity of luciferase was measured 48 hours later using the Dual-Luciferase
238 Assay System (Promega).
239
240 **Chromatin immunoprecipitation (ChIP) PCR**
241 ChIP assay was performed using the Simple ChIP Enzymatic Chromatin IP Kit (Magnetic Beads,
242 Cell Signaling Technology) according to the instructions. The ipsilateral dorsal horn of SNL- or

243 sham-operated mice was collected in 1% formaldehyde immediately to cross-link the proteins to
244 the DNA. After glycine treatment and PBS washing, the tissues were homogenized and lysed. The
245 chromatin was then collected and fragmented using enzymatic digestion. The disposed chromatin
246 was subjected to immunoprecipitation with normal IgG antibody (rabbit, 1:500; Cell Signaling
247 Technology, catalog #2729S, RRID: AB_1031062) as negative control (NC), histone H3 antibody
248 (rabbit, 1:50; Cell Signaling Technology, catalog #4620S, RRID: AB_1904005) as positive control,
249 DNMT3b antibody (mouse, 1:200; Abcam, catalog #ab13604, RRID: AB_300494), and KLF5
250 antibody (rabbit, 1:300; Millipore, catalog #07-1580, RRID: AB_1977308). The mixture was
251 captured by protein-G magnetic beads. After immunoprecipitation, the protein–DNA crosslinks
252 were reversed, and the DNA was purified. The enrichment of the *GPR151* promoter sequences
253 was measured through quantitative ChIP-PCR (qChIP-PCR) using the *DNMT3b* or *KLF5*
254 site-specific primer pairs in the *GPR151* promoter (Table 3). ChIP-PCR products were visualized
255 by GelRed (Biotium) staining in 3% agarose gels. As for qChIP-PCR, DNA samples and standards
256 were analyzed using FastStart Essential DNA Green Master for SYBR Green I based real-time
257 PCR (Roche Diagnostics) through the Light Cycler 96 Real-time PCR System (Roche
258 Diagnostics).
259

260 **In situ hybridization**

261 The template fragments of *GPR151* were amplified by PCR using primers (forward: 5' -CGG GAT
262 CCC GCA CGC AGG TGT GGA AAT GTG-3' and reverse: 5'-ACG AGC TCG CTG TCA TCA
263 GGA GAC CCA C-3') and subcloned into pSPT18. Digoxigenin (DIG)-labeled RNA antisense
264 and sense probes for the *GPR151* gene were synthesized using the DIG RNA Labeling Kit

(SP6/T7, Roche). Cellular localization of *GPR151* mRNA was performed using *in situ* hybridization assay kit (Boster Biological Technology, Wuhan, China). Briefly, the spinal cord sections and DRG sections (14 μm) were treated with 30% H_2O_2 and methanol (1:50) for 30 min at room temperature. After being washed with DEPC-treated ultrapure water, the sections were prehybridized at 42℃ for 4 hours at room temperature and hybridized with the DIG-labeled probe (1 μg/ml) in hybridization buffer at 42℃ overnight. After being washed by sodium chloride-sodium citrate buffer, sections were then incubated in blocking solution at 37℃ for 30 min and in mouse anti-DIG-biotin for 60 min at room temperature, washed with PBS (0.01 M, pH 7.4), and then incubated in SABC (Streptavidin-biotin complex)-Cy3 reagent (Boster Biological Technology) for 30 min at 37℃.

To further identify the cell types expressing GPR151 and the colocalization of GPR151 with KLF5 in the spinal cord, the sections under in situ hybridization were incubated overnight using primary antibodies against NeuN (mouse, 1:1000; Millipore, catalog #MAB377, RRID: AB_2298772), GFAP (mouse, 1:6000; Millipore, catalog #MAB360, RRID: AB_2275415), IBA-1 (rabbit, 1:3000; Wako, catalog #019-19741, RRID: AB_839504), and KLF5 (rabbit, 1:300; Millipore, catalog #07-1580, RRID: AB_1977308) and then further incubated with Alexa Fluor 488 goat anti-mouse IgG (H+L) or Alexa Fluor 488 goat anti-rabbit IgG (H+L) (Jackson ImmunoResearch) for 2 hours at room temperature. The signals were detected with Leica SP8 confocal microscope.

Immunohistochemistry

Animals were anesthetized with isoflurane and perfused through the ascending aorta with 0.9%

287 NaCl followed by 4% paraformaldehyde in 0.1 M PB. After perfusion, the L4-L5 spinal cord
288 segments were removed and postfixed in the same fixative 4-6 hours at 4°C. Spinal cord sections
289 (30 μm, free-floating) were cut in a cryostat and processed for immunofluorescence. The sections
290 were first blocked with 4% goat serum or donkey serum for 2 hours at room temperature and then
291 incubated overnight at 4°C with the following primary antibodies: Glial fibrillary acidic protein
292 (GFAP) (mouse, 1:6000; Millipore, catalog #MAB360, RRID: AB_2275415), NeuN (mouse,
293 1:1000; Millipore, catalog #MAB377, RRID: AB_2298772), CD11b (mouse, 1:50; Serotec,
294 catalog #MCA-257GA, RRID: AB_566455), IBA-1 (rabbit, 1:3000; Wako, catalog #019-19741,
295 RRID: AB_839504), KLF5 (rabbit, 1:300; Millipore, catalog #07-1580, RRID: AB_1977308),
296 calcitonin gene-related peptide antibody (CGRP) (mouse, 1:500; Sigma-Aldrich, catalog #C7113,
297 RRID: AB_259000), PKCγ (mouse, 1:500; Santa Cruz Biotechnology, catalog #sc-166451, RRID:
298 AB_2168997), and Isolectin B_4 (IB4) (1:50; Sigma-Aldrich, catalog #L2140, RRID:
299 AB_2313663). The sections were then incubated 2 hours at room temperature with Cy3- or Alexa
300 Fluor 488-conjugated secondary antibodies (1:1000; Jackson ImmunoResearch). For double
301 immunofluorescence, sections were incubated with a mixture of mouse and rabbit primary
302 antibodies followed by a mixture of Cy3- or Alexa Fluor 488- conjugated secondary antibodies.
303 The stained sections were examined with a Leica SP8 Gated STED confocal microscope (Leica
304 Microsystems, Wetzlar, Germany).
305

306 **Western blot**

307 Animals were perfused with 0.9% NaCl. Spinal cord tissues were homogenized in a RIPA lysis
308 buffer containing protease and phosphatase inhibitors (Roche). Protein samples (30 μg) were

309 separated on an SDS-PAGE gel and transferred to PVDF (Millipore) blots. The blots were blocked
310 with 5% skim milk in TBST and incubated with antibody against DNMT3B (goat, 1:300; Santa
311 Cruz Technology, catalog #sc-10236, RRID: AB_2094128), pERK (rabbit, 1:1000; Cell Signaling
312 Technology, catalog #9101, RRID: AB_331646), ERK (catalog #9102, RRID:AB_330744), pJNK
313 (catalog #9251, RRID: AB_331659), JNK (catalog #9252, RRID: AB_2250373), pp38 (catalog
314 #9211, RRID: AB_331641), and p38 (catalog #9212, RRID: AB_330713). The blots were further
315 incubated with GAPDH antibody (mouse, 1:20,000; Millipore, catalog #MAB374, RRID:
316 AB_2107445) for the control group. Then these bolts were incubated with IRDye 800CW Goat
317 Anti-Mouse IgG (H + L) (LI-COR Biosciences, catalog #P/N 925-32210, RRID: AB_2687825) or
318 IRDye 800CW Goat Anti-Rabbit IgG (H + L) (LI-COR Biosciences, catalog #925-32211, RRID:
319 AB_2651127) for 2 h at room temperature and displayed through Odyssey® CLx Imaging System
320 (LI-COR). Specific bands were evaluated by predicted molecular size, and the intensity of selected
321 bands was analyzed by ImageJ software (National Institutes of Health, RRID: SCR_003070).
322
323 **Microarray**
324 Total RNA was isolated from the L5 spinal cord at 10 days after SNL using the TRIzol reagent
325 (Invitrogen). There were 2 replicates for RNA samples from WT or *GPR151*$^{-/-}$ mice. Gene
326 expression profiles of the spinal cord were assessed with Agilent SurePrint G3 Mouse GE 8×60K
327 Microarray Kit (G4852A) by CapitalBio Corporation. Gene expression data of sham-operated
328 mice is from our previously reported data (Jiang et al., 2016).
329
330 **Lentiviral vectors production and intraspinal injection**

The shRNAs targeting murine *GPR151* (GenBank Accession: NM_181543.1. 5′-CCA TCA TTC CGT CTC TCT T-3′) and a negative control (NC) shRNA (5′-TTC TCC GAA CGT GTC ACG T-3′) were designed and inserted into lentiviral vector pGV248 which regulates the expression of shRNAs by the U6 promoter (LV-*GPR151* shRNA or LV-NC). The coding sequence of *DNMT3b* (GenBank Accession: NM_001122997.2) of mice was synthesized by Sangon Biotech (Shanghai, China) and cloned into pLV-Ubi-MCS-3FLAG to generate *DNMT3b*-expressing lentiviral plasmid, which mediated transcription of *DNMT3b* by ubiquitin promoter. Then the *DNMT3b*-expressing plasmid and EGFP-expressing plasmid (Control) were packaged into lentivirus. For the intraspinal injection, animals were anesthetized with isoflurane and carried out with hemilaminectomy at the L1-L2 vertebral segments. After exposure of the spinal cord, each animal received 2 injections (0.5 μl, 0.8 mm apart, and 0.5 mm deep) of the lentivirus (1×10^5 TU) along the L4-L5 dorsal root entry zone using a glass micropipette (diameter 60 μm). The tip of glass micropipette reached to the depth of lamina II-IV of the spinal cord. The dorsal muscle and skin were sutured. The intraspinal injection was performed unilaterally on the left side (Jiang et al., 2016).

Behavioral analysis

Animals were habituated to the testing environment daily for 2 days before baseline testing. All the testings were done by individuals blinded to the treatment or genotypes of the mice. In the tail immersion test, the temperature of the water was set at 48, 50, 52°C, and the tail flick latency was recorded. To test the hyperalgesia, the animals were put on a glass plate within a plastic box and allowed 30 min for habituation. Heat sensitivity was tested by radiant heat using Hargreaves apparatus (IITC model 390 Analgesia Meter, Life Science) which was expressed as paw

withdrawal latency. The latency baseline was adjusted to 10-14 s with a maximum of 20 s as cut off to prevent potential injury (Hargreaves et al., 1988). For mechanical allodynia, animals were put on an elevated metal mesh floor and allowed 30 min for habituation before an examination. The plantar surface of the hindpaw was stimulated with a series of von Frey hairs with logarithmically incrementing stiffness (0.02-2.56 grams, Stoelting, WoodDale, IL, USA) presented perpendicular to the plantar surface (2-3 s for each hair). The 50% paw withdrawal threshold was determined using Dixon's up-down method (Dixon, 1980). For the Rota-rod test, the speed was set at 10 rpm for 60 s and subsequently accelerated to 80 rpm within 5 min. The time for mice to fall after the beginning of the acceleration was recorded (Abbadie et al., 2003).

Experimental design and statistical analysis

All sample sizes and experimental design were based on previously published data from our lab and similar experiments in the field. All quantitative analysis were performed double-blinded. All data were expressed as mean ± SEM. The n number stands for the biological repeat. Each n number is indicated in the figures or the figure legends. All statistical analyses were performed using GraphPad Prism 5. Student's two-tailed t-test was used for two group comparisons, and one-way ANOVA or two-way repeated measures (RM) ANOVA was used for multi-group comparisons, followed by post-hoc Bonferroni tests. The criterion for statistical significance was $P < 0.05$. Details for statistical tests used were provided within figure legends or the results description.

Results

GPR151 expression is upregulated in spinal neurons after SNL

To search for novel GPCR genes and regulatory networks that are critical for the maintenance of neuropathic pain, we performed a genome-wide gene expression profiling analysis of the ipsilateral spinal cord dorsal horn 10 days after SNL (Jiang et al., 2015). Among all detectable oGPCR genes, 8 of them (*GPR151*, *GPR150*, *GPR84*, *GPR160*, *GPR124*, *GPR152*, *GPR174*, and *GPR160*) were up-regulated by more than 1.5-fold (Fig. 2A, B). Strikingly, *GPR151* was the most dramatically increased gene with a 26-fold increase ($p = 0.000$, Student's *t*-test, Fig. 2B).

We then checked the time course of *GPR151* expression in the ipsilateral dorsal horn after SNL or sham-operation by qPCR. *GPR151* mRNA was significantly increased at day 1, peaked at day 10, and maintained at day 21 in SNL mice ($F_{(4, 23)} = 12.152$, $p = 0.000$, one-way ANOVA, Fig. 2C). The mRNA level did not significantly differ between naïve and sham-operated mice at all the time points we checked ($F_{(4, 24)} = 1.850$, $p = 0.159$, one-way ANOVA, Fig. 2C).

To define the cellular localization of GPR151 in the spinal cord, we performed in situ hybridization using antisense probes for *GPR151* on spinal sections of SNL 10 days. The *GPR151*-positive signal was not shown in sections incubated with *GPR151* sense probe (Fig. 2D) but shown in sections with antisense probe (Fig. 2E). In situ hybridization combined with immunostaining showed that *GPR151* was primarily colocalized with neuronal marker NeuN (Fig. 2F), rarely with astrocytic marker GFAP (Fig. 2G), none with microglial marker IBA-1 (Fig. 2H). In lamina I-II and III-IV, 72.4 ± 4% and 73.2 ± 3% of NeuN-positive cells express GPR151, respectively. Single-cell RT-PCR analysis revealed co-expression of *GPR151* with NeuN in 3 of 4 neurons in lamina II (Fig. 2I). These data suggest the predominant expression of *GPR151* in spinal neurons.

397 We further characterized the type of *GPR151*$^{+}$ neurons. As somatostatin (SST) and GAD67
398 are respectively expressed in excitatory and inhibitory neurons (Zeilhofer et al., 2012; Duan et al.,
399 2014a), we performed *GPR151* in situ hybridization on *SST*-GFP^{+} or *GAD67*-GFP^{+} mice. It
400 showed that *GPR151* is expressed in *SST*-GFP^{+} neurons and *GAD67*-GFP^{+} neurons (Fig. 2J, K),
401 suggesting that *GPR151* is extensively expressed in dorsal horn neurons.

402 *GPR151* was reported to be highly increased in the DRG after CCI or burn injury (Reinhold
403 et al., 2015; Yin et al., 2016), we then checked *GPR151* expression in the DRG after SNL. As
404 shown in Fig. 2L, *GPR151* was dramatically increased at days 1 and 3, 10 and 21 after SNL ($F_{(4, 20)}$
405 $= 37.29$, $p = 0.000$, one-way ANOVA). In situ hybridization showed that GPR151 is expressed in
406 neuron-like cells in the DRG of naïve mice and increased after SNL (Fig. 2M-O).

407

408 **Mutation or inhibition of GPR151 persistently attenuates SNL-induced pain hypersensitivity**

409 To determine the role of GPR151 in pain sensation, *GPR151* mutant mice (*GPR151*$^{-/-}$) were
410 generated (Fig. 1 and Fig. 3A, B). *GPR151*$^{-/-}$ mice show normal distribution patterns of the
411 neuronal marker NeuN, astrocyte marker GFAP, microglia marker IBA-1 (Fig. 3C), and normal
412 innervations of the primary afferents, labeled with CGRP and IB4, and normal neurochemical
413 marker PKCγ in the spinal cord dorsal horn (Fig. 3D).

414 We further tested pain behaviors and motor function in wild-type (WT) and *GPR151*$^{-/-}$ mice
415 (Fig. 4A). Acute thermal sensitivity tested by hot water immersion and radiant heat, acute
416 mechanical sensitivity tested by von Frey, were indistinguishable in WT and *GPR151*$^{-/-}$ mice (Tail
417 flick test: $F_{(1,45)} = 0.06$, $p = 0.8126$, two-way ANOVA; Radiant heat test: $p = 0.924$, Student's *t*-test;
418 Von Frey test: $p = 0.6672$, Student's *t*-test). The rota-rod test revealed a similar falling latency in

WT and *GPR151*$^{-/-}$ mice (p = 0.6672, Student's *t*-test). These data indicate that *GPR151* mutation did not cause deficits in basal pain sensation and motor function.

Next, we tested pain behaviors after SNL. Consistent with previous reports (Jiang et al., 2016), SNL induced persistent mechanical allodynia (Fig. 4B) and heat hyperalgesia (Fig. 4C) in WT mice. However, SNL-induced mechanical allodynia was markedly reduced in *GPR151*$^{-/-}$ mice from 3 days to 42 days ($F_{(1, 88)}$ = 117.33, p = 0.000, two-way RM ANOVA, Fig. 4B). In addition, heat hyperalgesia was not developed in *GPR151*$^{-/-}$ mice in 42 days ($F_{(1, 88)}$ = 248.98, p = 0.000, two-way RM ANOVA, Fig. 4C).

To further investigate the role of spinal GPR151 in the maintenance of neuropathic pain, we intraspinally injected *GPR151* shRNA lentivirus (LV-*GPR151* shRNA) and control lentivirus (LV-NC) 5 days after SNL in WT mice. An *in vitro* study in HEK293 cells showed that the LV-*GPR151* shRNA reduced *GPR151* expression by 94.9 ± 0.5% compared to LV-NC (p = 0.000, Student's *t*-test, n=4/group). Intraspinal injection of LV-*GPR151* shRNA attenuated SNL-induced mechanical allodynia from 7 days to 63 days after SNL, and the second injection also effectively attenuated mechanical allodynia ($F_{(1, 162)}$ = 150.28, p = 0.000, two-way RM ANOVA, Fig. 4D). LV-*GPR151* shRNA treatment reversed SNL-induced heat hyperalgesia ($F_{(1, 81)}$ = 228.62, p = 0.000, two-way RM ANOVA, Fig. 4E). qPCR data showed that spinal injection of LV-*GPR151* shRNA reduced *GPR151* mRNA expression in lumbar segments by 42.8 ± 8.9% at SNL day 21, 40.0 ± 8.2% at day 63, and 15.9 ± 5.9% at SNL day 77 compared to LV-NC (Day 21: p = 0.032, Student's *t*-test, n=6 mice/group; Day 63: p = 0.008, Student's *t*-test, n=5 mice/group; Day 77: p = 0.084, Student's *t*-test, n=5 mice/group), confirming the knockdown effect of LV-*GPR151* shRNA at days 21 and 63. Collectively, the behavioral results obtained by different strategies suggest that GPR151

441 plays a pivotal role in the maintenance of neuropathic pain.

442

443 **Demethylation of the CpG sites of *GPR151* gene promoter after SNL**

444 DNA methylation is an essential epigenetic mechanism in controlling gene expression (Jaenisch,
445 2003). To determine how GRP151 expression is regulated, we examined the methylation status of
446 *GPR151* promoter region by methylation-specific PCR (MSP) and bisulfite sequencing PCR (BSP)
447 assays. The genomic structure of *GPR151* gene contains one CpG dinucleotides region with 10
448 CpG sites around the transcriptional starting site (TSS, Fig. 5A). The MSP assay showed that the
449 methylation of the *GPR151* promoter in the spinal cord dorsal horn of SNL mice was lower than
450 that in sham-operated mice (p = 0.020, Student's *t*-test, Fig. 5B). To further confirm the
451 methylation status of the 10 CpG sites within the *GPR151* promoter, DNA sequencing was
452 performed on PCR products of the 250 bp fragment obtained after the treatment of genomic DNA
453 samples with sodium bisulfite. As shown in Fig. 5C, all samples were successfully sequenced.
454 Consistent with the MSP assay, DNA methylation in CpG dinucleotides regions of *GPR151* gene
455 was decreased in SNL mice compared to sham-operated mice ($F_{(1, 40)} = 24.82$, $p = 0.000$, two-way
456 ANOVA, Fig. 5C, D).

457 The effect of DNA methylation on *GPR151* promoter activity was further analyzed in a cell
458 culture system using a coelenterazine-utilizing luciferase assay. The luciferase activity was not
459 different between transfection with methylated- and unmethylated-pCpG-free basic reporter vector
460 in HEK293 cells ($p > 0.05$, two-way ANOVA followed by Bonferroni posttests, Fig. 5E). However,
461 the activity was increased when the cells were transfected with unmethylated
462 pCpG-free-*GPR151*-promoter-Lucia vector compared to that transfected with methylated one ($p <$

0.001, two-way ANOVA followed by Bonferroni posttests, Fig. 5E), indicating that the promoter activity of mouse *GPR151* gene is increased by DNA demethylation.

DNMT3b is decreased after SNL and negatively regulates GPR151 expression and neuropathic pain

DNA methyltransferases (DNMTs), including DNMT1, DNMT3a, and DNMT3b, are important in directly regulating DNA methylation (Jurkowska et al., 2011). We previously found that the mRNA of *DNMT3b*, but not *DNMT1* or *DNMT3a* was decreased in the spinal cord after SNL (Jiang et al., 2017). Western blot showed that DNMT3b protein level was persistently reduced at days 1, 3, 10 and 21 after SNL ($F_{(4, 14)} = 0.08$, $p = 0.003$, one-way ANOVA, Fig. 5F). ChIP-PCR further showed that, after DNMT3b antibody immunoprecipitation, *GPR151* has lower enrichment of DNMT3b occupancy in the spinal cord of SNL mice compared to sham-treated mice ($p = 0.032$, Student's *t*-test, Fig. 5G), indicating that the binding of DNMT3b with the *GPR151* promoter is specific and is also reduced by SNL. These data also suggest that the down-regulated DNMT3b may be responsible for the demethylation of the *GPR151* promoter in neuropathic pain condition.

We then asked whether genetic silencing of DNMT3b activity could increase *GPR151* expression in naïve mice. Indeed, intrathecal administration of *DNMT3b* siRNA not only decreased the spinal *DNMT3b* mRNA level ($p = 0.010$, Student's *t*-test), also dramatically increased *GPR151* mRNA expression 3 days after injection ($p = 0.009$, Student's *t*-test, Fig. 5H). Meanwhile, the methylation level of the *GPR151* promoter was reduced ($p = 0.007$, Student's *t*-test, Fig. 5I). The behavioral study showed that intrathecal injection of *DNMT3b* siRNA in naïve mice induced mechanical allodynia at days 2 and 3 after treatment ($F_{(1, 65)} = 17.37$, $p = 0.000$,

two-way RM ANOVA, Fig. 5J). Based on the behavioral results, we further checked the mRNA level of *DNMT3b* and *GPR151* 2 days and 4 days after siRNA injection. The results showed that DNMT3b mRNA was decreased [0.62 ± 0.08 (*DNMT3b* siRNA) vs. 1 ± 0.12 (NC), $p = 0.027$] and *GPR151* mRNA was increased at day 2 [1.36 ± 0.14 (*DNMT3b* siRNA) vs. 1 ± 0.02 (NC), $p = 0.030$, Student's t-test, n=5 mice/group], but not at day 4 [*DNMT3b*: 0.78 ± 0.10 (*DNMT3b* siRNA) vs. 1 ± 0.10 (NC), $p = 0.139$; *GPR151*: 0.88 ± 0.08 (*DNMT3b* siRNA) vs. 1 ± 0.03 (NC), $p = 0.182$, Student's t-test, n=5 mice/group]. Furthermore, intraspinal injection of *DNMT3b*-expressing lentivirus (LV-*DNMT3b*) effectively increased *DNMT3b* expression ($p = 0.001$, Student's *t*-test, Fig. 5K), reduced *GPR151* expression $p = 0.000$, Student's *t*-test, Fig. 5K), and increased the methylation of *GPR151* promoter ($p = 0.016$, Student's *t*-test, Fig. 5L). Consistently, injection of LV-*DNMT3b* 3 days before SNL alleviated SNL-induced mechanical allodynia at days 14, 21 and 28 after SNL ($F_{(1, 77)} = 34.47$, $p = 0.000$, two-way RM ANOVA, Fig. 5M). These data indicate the negative regulation of DNMT3b on *GPR151* methylation and the involvement of DNMT3b in the pathogenesis of neuropathic pain.

KLF5 leads to transactivation of the *GPR151* gene promoter after SNL

DNA methylation can regulate transcription by interfering with transcription factor binding (Poetsch and Plass, 2011). To reveal the transcriptional factors that may regulate *GPR151* expression, the sequence from -1500 to +500 of *GPR151* promoter was analyzed. Five KLF5 binding sites, 2 STAT3 binding sites, and 2 NFATC2 binding sites (Fig. 6A-C) were predicted within *GPR151* promoter region based on JASPAR CORE in Vertebrata with a defined 80% profile score threshold (http://jaspar.genereg.net/). A conservation analysis using the UCSC

genome browser showed that the 5 binding sites of KLF5 are well conserved among mouse, rat, and human (data not shown).

We then examined the binding of KLF5 with *GPR151* promoter in the spinal cord dorsal horn after SNL by ChIP-PCR. After KLF5 antibody immunoprecipitation, the ChIP-PCR analysis revealed that *GPR151* promoter has higher enrichment of KLF5 occupancy in the spinal cord of SNL mice compared to sham mice (p = 0.030, Student's *t*-test, Fig. 6D), indicating that the binding of KLF5 with the *GPR151* promoter in the spinal cord is enhanced by SNL.

To determine the effect of KLF5 on *GPR151* expression, we conducted a luciferase activity assay in vitro. KLF5-expressing vector and pCpG-free-*GPR151*-promoter-Lucia vector (methylated or unmethylated) were cotransfected. As shown in Fig. 6E, in HEK293 cells transfected with methylated pCpG-free-*GPR151*-promoter-Lucia vector, co-transfection with KLF5-expressing vector slightly increased the promoter luciferase activity, compared to the absence of KLF5-expressing vector. However, in these cells transfected with unmethylated pCpG-free-*GPR151*-promoter-Lucia vector, co-transfection of KLF5-expressing vector dramatically increased the luciferase activity, compared to the absence of KLF5-expressing vector. In addition, KLF5 induced more luciferase activity increase in cells transfected with unmethylated pCpG-free-*GPR151*-promoter-Lucia vector than transfected with methylated one ($F_{(1, 12)}$ = 1030, p = 0.000, two-way ANOVA, Fig. 6E). These results suggest that KLF5 increases the transcription of the *GPR151* gene, which is further enhanced when *GPR151* promoter is demethylated.

To examine which binding site(s) of KLF5 on GPR151 promoter is essential for *GPR151* gene expression, we made site-directed mutagenesis of putative KLF5 consensus binding sites for the *GPR151* promoter (Fig. 6F). KLF5 vector (0.5 μg/well in 6-well plates) was co-transfected

529 into HEK293 cells with mutant constructs and Renilla. The results from promoter assays showed
530 that mutation of binding site-1 (BS1), site-2 (BS2) or site-5 (BS5) did not significantly change the
531 transcription activity of KLF5, but mutation of binding site-3 (BS3) or site-4 (BS4) almost
532 completely blocked the transactivation effect of KLF5 ($F_{(6, 27)} = 11.99$, $p = 0.000$, one-way
533 ANOVA, Fig. 6F). These results further confirm that KLF5 facilitates the up-regulation of
534 *GPR151,* and also suggest that the third and fourth KLF5 binding sites in the *GPR151* promoter
535 are responsible for KLF5-mediated transcriptional activation.
536
537 **SNL increases KLF5 expression in spinal neurons**
538 We then examined KLF5 expression in the spinal cord dorsal horn after SNL. RT-PCR showed
539 that *KLF5* mRNA was significantly increased at days 1, 3, 10, and 21 after SNL ($F_{(4, 28)} = 7.585$, p
540 $= 0.000$, one-way ANOVA, Fig. 7A). Immunostaining showed that KLF5 had a low basal
541 expression in the superficial dorsal horn in naïve mice (Fig. 7B), and was markedly increased in
542 the ipsilateral dorsal horn 10 days after SNL (Fig. 7C). Besides, the KLF5-positive signal was
543 mostly colocalized with NeuN (Fig. 7D), partially with GFAP (Fig. 7E), but not with CD11b (Fig.
544 7F) in the dorsal horn of spinal cord. Furthermore, KLF5 is highly colocalized with *GPR151* (Fig.
545 7G). The staining of KLF5 on the sections from *SST*-GFP$^+$ or *GAD67*-GFP$^+$ mice showed that
546 KLF5 is expressed in *SST*-GFP$^+$ neurons (Fig. 7H) and *GAD67*-GFP$^+$ neurons (Fig. 7I). These data
547 indicate the predominant expression of KLF5 in GPR151$^+$ neurons.
548
549 ***KLF5* siRNA attenuates SNL-induced pain hypersensitivity and decreases *GPR151***
550 **expression in the spinal cord**

To determine whether KLF5 plays a role in the maintenance of SNL-induced neuropathic pain, we intrathecally injected *KLF5* or NC siRNA 10 days after SNL. Behavioral data showed that *KLF5* siRNA dramatically attenuated SNL-induced mechanical allodynia from 6 to 24 h after injection ($F_{(1, 66)} = 9.93$, $p = 0.002$, two-way RM ANOVA, Fig. 7J). Meanwhile, *KLF5* siRNA also attenuated SNL-induced heat hyperalgesia ($F_{(1, 66)} = 9.07$, $p = 0.004$, two-way RM ANOVA, Fig. 7K). To examine the knockdown effect of *KLF5* siRNA, we checked the mRNA level in another set of animals 24 h after SNL. As shown in Fig. 7L, *KLF5* siRNA reduced *KLF5* ($p = 0.034$, Student's *t*-test) and *GPR151* mRNA ($p = 0.010$, Student's *t*-test) expression in the spinal cord.

To further confirm the role of KLF5 in neuropathic pain, ML264, a potent and selective KLF5 inhibitor, was intrathecally injected 10 days after SNL. ML264 at the dose of 1 nmol did not affect mechanical allodynia, but 10 nmol ML264 increased the threshold at 24 h ($F_{(2, 68)} = 8.106$, $p = 0.001$, two-way RM ANOVA, Fig. 7M). For the thermal test, ML264 at the dose of 1 nmol alleviated SNL-induced heat hyperalgesia at 24 and 48 h (Fig. 7N). The higher dose (10 nmol) reversed SNL-induced heat hyperalgesia at 24 h ($F_{(2, 68)} = 24.5$, $p = 0.000$, two-way RM ANOVA, Fig. 7N). The treatment also reduced the expression of *KLF5* and *GPR151* (Fig. 7O). These results suggest that KLF5 regulates GPR151 expression and is involved in SNL-induced neuropathic pain.

Mutation of *GPR151* decreases the expression of MAPK pathway-related genes and the activation of ERK in the spinal cord after SNL

To investigate the downstream signaling of GPR151 activation, we performed microarray to compare gene expression in the spinal cord of *GPR151*$^{-/-}$ and WT mice. First, we obtained a

573 graphical overview of the expression signatures of mRNAs using a scatter plot. It showed that a
574 large number of mRNAs were differentially expressed between *GPR151*$^{-/-}$ and WT mice (Fig. 8A).
575 In the differentially expressed mRNAs, there were 616 genes whose mRNA change was more than
576 1.5-fold. Among them, 38 genes were downregulated, and 227 genes were upregulated in
577 *GPR151*$^{-/-}$ mice. The heat map generated with the values for all the differentially expressed genes
578 showed that *GPR151*$^{-/-}$-SNL and WT-Sham samples clustered together (Fig. 8B), suggesting that
579 the transcript values for *GPR151*$^{-/-}$-SNL mice were closer to the values obtained from WT-sham
580 mice than those from WT-SNL mice. We further performed cluster analysis of expression values
581 for the set of pain-related genes from Pain Gene Database (Lacroix-Fralish et al., 2007).
582 Expression levels of multiple genes in the algogenic pain processing pathway were decreased in
583 *GPR151*$^{-/-}$-SNL mice compared with WT-SNL group. These genes include colony stimulating
584 factor 2 receptor beta common subunit (*CSF2RB*), interleukin 1 beta (*IL1B*), interleukin 1 receptor
585 type 1 (*IL1R1*), G protein-coupled receptor 84 (*GPR84*), C-X-C motif chemokine ligand 13
586 (*CXCL13*), toll-like receptor 2 (*TLR2*), toll-like receptor 4 (*TLR4*), purinergic receptor P2Y12
587 (*P2RY12*), and interferon regulatory factor 8 (*IRF8*) (Fig. 8C). Several analgesic genes were
588 increased in *GPR151*$^{-/-}$-SNL mice, including G protein-coupled receptor kinase 2 (*GRK2*), dual
589 specificity phosphatase 6 (*DUSP6*), superoxide dismutase 2 (*SOD2*), arrestin beta 2 (*ARRB2*), ST8
590 alpha-N-acetyl-neuraminide alpha-2, 8-sialyltransferase 1 (*ST8SIA1*), gamma-aminobutyric acid
591 type B receptor subunit 1 (*GABBR1*), opioid receptor mu 1 (*OPRM1*), and solute carrier family 12
592 member 2 (*SLC12A2*) (Fig. 8D). These data suggest that mutation of *GPR151* changes the
593 expression of many genes associated with neuropathic pain.

594 To explore the molecular pathways mediated by *GPR151* in the spinal cord, we performed

KEGG pathway analysis. As shown in Fig. 8E, KEGG analysis of down-regulated genes showed that 6 KEGG pathways were downregulated in the absence of *GPR151*, including MAPK signaling, calcium signaling, focal adhesion, insulin signaling, taste transduction, and cytokine-cytokine receptor interaction. Upregulated genes in *GPR151*$^{-/-}$-SNL mice involved retinol metabolism, complement and coagulation cascades, drug metabolism-cytochrome P450, ECM-receptor interaction, focal adhesion, and cell communication pathways (Fig. 8F). Based on the important role of MAPK signaling in neuropathic pain (Ji et al., 2009), we validated the MAPK signaling pathway genes by qPCR. We checked the expression of fibroblast growth factor 14 (*FGF14*) (p = 0.01, Student's *t*-test), protein kinase cAMP-activated catalytic subunit alpha (*PRKACA*) (p = 0.019, Student's *t*-test), CRK proto-oncogene adaptor protein (*CRK*) (p = 0.029, Student's *t*-test), mitogen-activated protein kinase kinase kinase 13 (*MAP3K13*) (p = 0.012, Student's *t*-test), and growth factor receptor bound protein 2 (*GRB2*) (p = 0.025, Student's *t*-test, Fig. 8G) and found that they were significantly reduced in the spinal cord of *GPR151*$^{-/-}$ mice, compared to that in WT mice (Fig. 8G). We also assessed levels of phosphorylation of the three MAPK family members: extracellular signal-regulated kinase (ERK), p38, and c-Jun N-terminal kinase (JNK) (Fig. 8H, I). Interestingly, the phosphoERK (pERK) was substantially inhibited by *GPR151* ablation (p = 0.043, *GPR151*$^{-/-}$-SNL vs. WT-SNL, Student's *t*-test), and pp38 expression was increased in both WT and *GPR151*$^{-/-}$ mice (p = 0.021, WT-SNL vs. WT-Sham; p = 0.017 *GPR151*$^{-/-}$-SNL vs. *GPR151*$^{-/-}$-Sham, Student's *t*-test), whereas pJNK expression was not changed after SNL in both WT and *GPR151*$^{-/-}$ mice (p = 0.693, WT-SNL vs. WT-Sham; p = 0.688, *GPR151*$^{-/-}$-SNL vs. *GPR151*$^{-/-}$-Sham, Student's *t*-test). The above results suggest that GPR151 may contribute to the maintenance of neuropathic pain via downregulating algogenic genes, especially MAPK signaling pathway-related

genes.

Discussion

The development and maintenance of neuropathic pain is a process involving morphological, functional, and transcriptional changes in the nervous system. The mechanisms and the key transcriptional regulators controlling the pain-related gene expression are not well understood on the molecular level. Emerging evidence showed that orphan GPCRs are involved in the initiation and progression of neuropathic pain (Nicol et al., 2015; Li et al., 2017b). Our results strongly suggest that spinal GPR151 contributes to neuropathic pain genesis. Mechanistically, SNL increases *GPR151* expression by decreasing DNMT3b expression, preventing the maintenance of promoter DNA methylation, and increasing KLF5 expression and recruitment. Additionally, the increased GPR151 may participate in neuropathic pain via activating the MAPK pathway and increasing algogenic pain genes expression (Fig. 9). Thus, our results reveal a significant role of GPR151 in mediating neuropathic pain and the epigenetic mechanism underlying GPR151 expression.

GPCRs are the predominant receptors of neuromodulators and regulate a wide range of nervous system disorders and diseases including anxiety, schizophrenia, epilepsy, Alzheimer's disease, Parkinson's disease, and chronic pain (Baulac et al., 2001; Ahmed et al., 2010; Gaillard et al., 2014; Masseck et al., 2014; Hao et al., 2015; Foster and Conn, 2017; Xie et al., 2017). About 100 orphan GPCRs have been identified to be potential targets for the therapeutics of nervous system diseases (Civelli, 2012). Although the search for their endogenous ligands has been a challenge, the development of molecular biology and gene knockout techniques made the

639 identification of orphan GPCRs functions amenable (Cui et al., 2016; Chang et al., 2017;
640 Khrimian et al., 2017). Several studies have recently demonstrated that orphan GPCRs in the
641 spinal cord are critical players in the induction and maintenance of pathological pain (Nicol et al.,
642 2015; Li et al., 2017b). Especially, GPR84 is increased in the sciatic nerve and spinal cord after
643 partial sciatic ligation, mediates pain hypersensitivity via the modulation of peripheral
644 macrophage response (Nicol et al., 2015). Consistent with this observation, our data also revealed
645 the increase of *GPR84* in the spinal cord after SNL. Interestingly, among all the detected GPCR
646 genes, *GPR151* was the most markedly increased GPCR with a 26-fold increase. qPCR confirmed
647 the increase of *GPR151* from day 3 to day 21 after SNL. Previous studies have shown that
648 GPR151 was exclusively expressed in neurons of habenula (Kobayashi et al., 2013; Broms et al.,
649 2015). Our results also showed predominant expression of GPR151 in neurons of lamina I-IV of
650 the dorsal horn. Furthermore, GPR151 was expressed in both SST^+-excitatory neurons and
651 $GAD67^+$-inhibitory neurons in lamina II. Recent studies showed that ablation of SST^+ neurons
652 causes loss of mechanical pain, whereas ablation of dynorphin neurons (> 80% in $GAD67^+$
653 neurons) induces spontaneous mechanical allodynia (Duan et al., 2014b). Taken with the
654 behavioral results (Fig. 4D-G), we speculate that GPR151 in excitatory neurons of lamina II and
655 projection neurons of lamina I and III-IV may play a significant role in the pathogenesis of
656 neuropathic pain, which needs further investigation.

657 Behavioral studies showed that *GPR151* mutation did not affect basal pain, which is
658 consistent with the recent report (Holmes et al., 2016). However, Holmes et al. showed that
659 GPR151 was highly upregulated after SNI, but deletion of GPR151 did not affect SNI-induced
660 neuropathic pain. It is possible that different gene mutation strategy (Deletion mutation vs.

661 Insertion mutation) or different nerve injuries used (SNL vs. SNI) affects the phenotype, and
662 GPR151 in the DRG may not contribute to neuropathic pain (Holmes et al., 2016). We used
663 LV-*GPR151* shRNA to specific knockdown GPR151 in the spinal cord and found that
664 SNL-induced mechanical allodynia was persistently attenuated and even the second injection of
665 LV-*GPR151* shRNA was still effective in reversing late-phase neuropathic pain. These data
666 support the involvement of spinal GPR151 in the development and maintenance of neuropathic
667 pain.

668 A growing body of evidence has suggested that aberrant epigenetic changes are one of the
669 most frequent events and are regarded as important mechanisms in neuropathic pain (Zhang et al.,
670 2011a; Imai et al., 2013; Hong et al., 2015; Laumet et al., 2015). DNA demethylation has an
671 essential role in regulating pain-related gene expression (Zhang et al., 2015; Jiang et al., 2017;
672 Zhao et al., 2017). We identified *GPR151* as a novel preferentially demethylated gene after SNL.
673 Moreover, the demethylation of *GPR151* is positively associated with the persistent decrease of
674 DNMT3b in the spinal cord. Manipulation of *DNMT3b* expression by siRNA or over-expression
675 lentivirus changed the DNA methylation level of the *GPR151* promoter and GPR151 expression.
676 DNMT3b is a crucial de novo methyltransferase, preferentially expressed in neurons within the
677 nervous system (Pollemamays et al., 2014). Furthermore, DNMT3b can aggravate neurological
678 disorders progression through demethylation of target genes' promoter by downregulation of itself
679 (Das et al., 2010; Hui et al., 2015). Recent studies showed that DNMT3b was decreased in the
680 DRG and downregulated the methylation level of *P2X3R* gene promoter and enhanced interaction
681 with NFκB in cancer pain and diabetes pain models in rats (Zhang et al., 2015; Zhou et al., 2015).
682 Our previous work demonstrated that the expression of *DNMT3b* mRNA was remarkably

683 downregulated in the spinal cord in SNL mice, which contributed to the demethylation of
684 chemokine receptor *CXCR3* promoter (Jiang et al., 2017). Therefore, SNL-induced
685 downregulation of DNMT3b in the DRG and spinal cord may affect the expression of a variety of
686 genes, including GPR151.

687 DNA methylation and transcription factors usually work together to regulate gene expression
688 (Zhang et al., 2015; Guhathakurta et al., 2017; Li et al., 2017a; Yu et al., 2017). Under
689 physiological conditions, several transcription factors, such as Runx1, IRF5, C/EBPβ, ZFHX2,
690 have been demonstrated to participate in the gating of pain via activating the expression of
691 nociceptive genes (Lou et al., 2013; Masuda et al., 2014; Habib et al., 2017; Qi et al., 2017). We
692 showed that following SNL, KLF5 was increased in the spinal neuron, and contributed to
693 *GPR151* upregulation via direct binding to the promoter loci of *GPR151* and increasing its
694 transcription. KLF5 is a member of the large KLF family of transcription factors and has been
695 found localized in the neurons of hippocampus and hypothalamus, where it plays vital parts in the
696 pathogenesis of schizophrenia and food intake, respectively (Yanagi et al., 2008; Moore et al.,
697 2011; Kojima et al., 2013). Previous reports have shown that inhibiting KLF6, KLF9, and
698 KLF15 by DNA decoys produces a long-term pain treatment in rat models of neuropathic pain
699 (Mamet et al., 2017b). We provide the first evidence that inhibition of KLF5 through intrathecal
700 injection of siRNA or chemical inhibitor effectively attenuated pain hypersensitivity and inhibited
701 *GPR151* increase. In addition, DNMT3b-mediated DNA demethylation is essential for the binding
702 of KLF5 on the target sites in the *GPR151* promoter. However, it is worth noting that KLF5 may
703 also be involved in neuropathic pain via targeting genes other than *GPR151* (Drosatos et al., 2016).
704 GPR151 may also be regulated by other transcription factors, such as STAT3, NFATC2, which

705 also can bind on the GPR151 promoter.

706 Our array data revealed that mutation of *GPR151* has a vital function in genome-wide
707 gene-expression changes in the spinal cord caused by SNL. SNL changes the expression of a vast
708 amount of functional genes, such as ion channels, GPCRs, and kinases in the spinal cord
709 (Lacroix-Fralish et al., 2011; Jiang et al., 2015). Notably, our transcriptome analysis data showed
710 that mutation of *GPR151* normalized the expression profile of differentially expressed genes after
711 nerve injury. Moreover, mutation of *GPR151* downregulated algogenic genes' expression and
712 upregulated analgesic genes' expression after nerve injury, which may contribute to the reduced
713 hypersensitivity to mechanical or thermal stimuli. *GPR151* mutation also impaired the expression
714 of MAPK signaling pathway associated genes *FGF14, PRKACA, CRK, MAP3K13* and GRB2 in
715 the spinal cord after SNL. These genes may decrease the signal intensity of MAPK signaling
716 pathway. Several lines of evidence strongly suggest that spinal MAPK signaling play a pivotal role
717 in the development of inflammatory and neuropathic pain (Ji et al., 2009; Edelmayer et al., 2014).
718 Previous reports have shown that P38 and JNK are respectively activated in spinal microglia and
719 astrocytes, while ERK is activated in spinal neurons, astrocytes, and microglia after nerve injury in
720 rats (Jin et al., 2003; Zhuang et al., 2005; Zhuang et al., 2006; Jiang et al., 2016). Our Western blot
721 data showed that SNL-induced p38 activation was not affected by *GPR151* ablation, and JNK was
722 not activated in C57BL/6 background WT mice and *GPR151*$^{-/-}$ mice after SNL. However,
723 SNL-induced ERK was substantially inhibited by *GPR151* ablation, suggesting that ERK is an
724 important downstream of GPR151. In addition, ERK has been identified to be a downstream
725 kinase of Gαi-subunit containing GPCRs (Goldsmith and Dhanasekaran, 2007). Whether GPR151
726 is a Gαi-coupled receptor needs further investigation.

In conclusion, we provide the first evidence that SNL increased GPR151 expression via DNMT3b-mediated demethylation of the GRP151 promoter and KLF5-mediated increase of *GPR151* transcription. Also, GPR151 contribute to the maintenance of neuropathic pain, probably via activating the ERK signaling pathway. Thus, GPR151 may be a potentially novel therapeutic target for the alleviation of neuropathic pain.

749 **References**

750 Abbadie C, Lindia JA, Cumiskey AM, Peterson LB, Mudgett JS, Bayne EK, Demartino JA, Macintyre DE,
751 Forrest MJ (2003) Impaired Neuropathic Pain Responses in Mice Lacking the Chemokine
752 Receptor CCR2. Proceedings of the National Academy of Sciences of the United States of
753 America 100:7947-7952.
754 Ahmed MR, Berthet A, Bychkov E, Porras G, Li Q, Bioulac BH, Carl YT, Bloch B, Kook S, Aubert I (2010)
755 Lentiviral overexpression of GRK6 alleviates L-dopa-induced dyskinesia in experimental
756 Parkinson's disease. Science Translational Medicine 2:28ra28.
757 Anand P, Shenoy R, Palmer JE, Baines AJ, Lai RYK, Robertson J, Bird N, Ostenfeld T, Chizh BA (2011)
758 Clinical trial of the p38 MAP kinase inhibitor dilmapimod in neuropathic pain following nerve
759 injury. Eur J Pain 15:1040-1048.
760 Baulac S, Huberfeld G, Gourfinkelan I, Mitropoulou G, Beranger A, Prud'Homme JF, Baulac M, Brice A,
761 Bruzzone R, Leguern E (2001) First genetic evidence of GABA(A) receptor dysfunction in
762 epilepsy: a mutation in the gamma2-subunit gene. Nature Genetics 28:46.
763 Broms J, Antolinfontes B, Tingström A, Ibañeztallon I (2015) Conserved expression of the GPR151
764 receptor in habenular axonal projections of vertebrates. Journal of Comparative Neurology
765 523:359.
766 Broms J, Grahm M, Haugegaard L, Blom T, Meletis K, Tingström A (2017) Monosynaptic retrograde
767 tracing of neurons expressing the G‐protein coupled receptor Gpr151 in the mouse brain.
768 Journal of Comparative Neurology 525.
769 Cedar H, Bergman Y (2012) Programming of DNA methylation patterns. Annual Review of Biochemistry
770 81:97.
771 Chang J, Mancuso MR, Maier C, Liang X, Yuki K, Lu Y, Kwong JW, Jing W, Rao V, Vallon M (2017) Gpr124
772 is essential for blood-brain barrier integrity in central nervous system disease. Nat Med
773 23:450.
774 Civelli O (2012) Orphan GPCRs and Neuromodulation. Neuron 76:12-21.
775 Cui J, Ding Y, Chen S, Zhu X, Wu Y, Zhang M, Zhao Y, Li TR, Sun LV, Zhao S (2016) Disruption of Gpr45
776 causes reduced hypothalamic POMC expression and obesity. Journal of Clinical Investigation
777 126:3192.
778 Das S, Foley N, Bryan K, Watters KM, Bray I, Murphy DM, Buckley PG, Stallings RL (2010) MicroRNA
779 Mediates DNA Demethylation Events Triggered by Retinoic Acid during Neuroblastoma Cell
780 Differentiation. Cancer Research 70:7874-7881.
781 Dixon WJ (1980) Efficient analysis of experimental observations. Annual Review of Pharmacology &
782 Toxicology 20:441.
783 Drosatos K, Pollak NM, Pol CJ, Ntziachristos P, Willecke F, Valenti MC, Trent CM, Hu YY, Guo SD, Aifantis
784 I, Goldberg IJ (2016) Cardiac Myocyte KLF5 Regulates Ppara Expression and Cardiac Function.
785 Circ Res 118:241-253.
786 Duan B, Cheng LZ, Bourane S, Britz O, Padilla C, Garcia-Campmany L, Krashes M, Knowlton W,
787 Velasquez T, Ren XY, Ross SE, Lowell BB, Wang Y, Goulding M, Ma QF (2014a) Identification of
788 Spinal Circuits Transmitting and Gating Mechanical Pain. Cell 159:1417-1432.
789 Duan B, Cheng L, Bourane S, Britz O, Padilla C, Garcia-Campmany L, Krashes M, Knowlton W, Velasquez
790 T, Ren X, Ross SE, Lowell BB, Wang Y, Goulding M, Ma Q (2014b) Identification of spinal
791 circuits transmitting and gating mechanical pain. Cell 159:1417-1432.

792 Edelmayer RM, Brederson JD, Jarvis MF, Bitner RS (2014) Biochemical and pharmacological assessment
793 of MAP-kinase signaling along pain pathways in experimental rodent models: a potential tool
794 for the discovery of novel antinociceptive therapeutics. Biochemical pharmacology
795 87:390-398.
796 Foster DJ, Conn PJ (2017) Allosteric Modulation of GPCRs: New Insights and Potential Utility for
797 Treatment of Schizophrenia and Other CNS Disorders. Neuron 94:431-446.
798 Gaillard S, Lo Re L, Mantilleri A, Hepp R, Urien L, Malapert P, Alonso S, Deage M, Kambrun C, Landry M
799 (2014) GINIP, a Gαi-Interacting Protein, Functions as a Key Modulator of Peripheral GABAB
800 Receptor-Mediated Analgesia. Neuron 84:123-136.
801 Goldsmith ZG, Dhanasekaran DN (2007) G protein regulation of MAPK networks. Oncogene
802 26:3122-3142.
803 Guhathakurta S, Bok E, Evangelista BA, Kim YS (2017) Deregulation of α-synuclein in Parkinson's
804 disease: Insight from epigenetic structure and transcriptional regulation of SNCA. Progress in
805 Neurobiology.
806 Habib AM, Matsuyama A, Okorokov AL, Santana-Varela S, Bras JT, Aloisi AM, Emery EC, Bogdanov YD,
807 Follenfant M, Gossage SJ (2017) A novel human pain insensitivity disorder caused by a point
808 mutation in ZFHX2. Brain : a journal of neurology.
809 Hao JR, Sun N, Lei L, Li XY, Yao B, Sun K, Hu R, Zhang X, Shi XD, Gao C (2015) L-Stepholidine rescues
810 memory deficit and synaptic plasticity in models of Alzheimer's disease via activating
811 dopamine D1 receptor/PKA signaling pathway. Cell Death & Disease 6:e1965.
812 Hargreaves K, Dubner R, Brown F, Flores C, Joris J (1988) A new and sensitive method for measuring
813 thermal nociception in cutaneous hyperalgesia. Pain 32:77-88.
814 Hauser A, Chavali S, Masuho I, Jahn L, Martemyanov K, Gloriam D, Babu M (2017) Pharmacogenomics
815 of GPCR Drug Targets. Cell.
816 Hehn CAV, Baron R, Woolf CJ (2012) Deconstructing the Neuropathic Pain Phenotype to Reveal Neural
817 Mechanisms. Neuron 73:638.
818 Holmes FE, Kerr N, Chen YJ, Vanderplank P, Mcardle CA, Wynick D (2016) Targeted disruption of the
819 orphan receptor Gpr151 does not alter pain-related behaviour despite a strong induction in
820 dorsal root ganglion expression in a model of neuropathic pain. Molecular & Cellular
821 Neurosciences 78:35-40.
822 Hong S, Zheng G, Wiley JW (2015) Epigenetic regulation of genes that modulate chronic stress-induced
823 visceral pain in the peripheral nervous system. Gastroenterology 148:148-157.
824 Hui L, Qiu H, Yang J, Ni J, Le W (2015) Chronic hypoxia facilitates Alzheimer's disease through
825 demethylation of γ-secretase by downregulating DNA methyltransferase 3b. Alzheimers &
826 Dementia 12:130-143.
827 Ignatov A, Hermans-Borgmeyer I, Schaller HC (2004) Cloning and characterization of a novel
828 G-protein-coupled receptor with homology to galanin receptors. Neuropharmacology
829 46:1114-1120.
830 Imai S, Ikegami D, Yamashita A, Shimizu T, Narita M, Niikura K, Furuya M, Kobayashi Y, Miyashita K,
831 Okutsu D (2013) Epigenetic transcriptional activation of monocyte chemotactic protein 3
832 contributes to long-lasting neuropathic pain. Brain A Journal of Neurology 136:828-843.
833 Jaenisch R (2003) Epigenetic regulation of gene expression: how the genome integrates intrinsic and
834 environmental signals.
835 Ji RR, Th GR, Malcangio M, Strichartz GR (2009) MAP kinase and pain. Brain Research Reviews 60:135.

836 Jiang BC, Sun WX, He LN, Cao DL, Zhang ZJ, Gao YJ (2015) Identification of lncRNA expression profile in
837 the spinal cord of mice following spinal nerve ligation-induced neuropathic pain. Mol Pain 11.
838 Jiang BC, Cao DL, Zhang X, Zhang ZJ, He LN, Li CH, Zhang WW, Wu XB, Berta T, Ji RR (2016) CXCL13
839 drives spinal astrocyte activation and neuropathic pain via CXCR5. Journal of Clinical
840 Investigation 126:745.
841 Jiang BC, He LN, Wu XB, Shi H, Zhang WW, Zhang ZJ, Cao DL, Li CH, Gu J, Gao YJ (2017) Promoted
842 Interaction of C/EBP alpha with Demethylated Cxcr3 Gene Promoter Contributes to
843 Neuropathic Pain in Mice. Journal of Neuroscience 37:685-700.
844 Jin SX, Zhuang ZY, Woolf CJ, Ji RR (2003) p38 mitogen-activated protein kinase is activated after a
845 spinal nerve ligation in spinal cord microglia and dorsal root ganglion neurons and contributes
846 to the generation of neuropathic pain. Journal of Neuroscience the Official Journal of the
847 Society for Neuroscience 23:4017-4022.
848 Jurkowska RZ, Jurkowski TP, Jeltsch A (2011) Structure and Function of Mammalian DNA
849 Methyltransferases. Chembiochem 12:206-222.
850 Khrimian L, Obri A, Ramosbrossier M, Rousseaud A, Moriceau S, Nicot AS, Mera P, Kosmidis S,
851 Karnavas T, Saudou F (2017) Gpr158 mediates osteocalcin's regulation of cognition. Journal of
852 Experimental Medicine 214:2859.
853 Kobayashi Y, Sano Y, Vannoni E, Goto H, Suzuki H, Oba A, Kawasaki H, Kanba S, Lipp HP, Murphy NP
854 (2013) Genetic dissection of medial habenula–interpeduncular nucleus pathway function in
855 mice. Frontiers in behavioral neuroscience 7:17.
856 Kojima T, Manabe I, Nagai R, Komuro I (2013) SUMOylation of KLF5 controls food intake by suppressing
857 AgRP expression on contact with FoxO1 in hypothalamic neurons. European Heart Journal
858 34:780-780.
859 Lacroix-Fralish ML, Ledoux JB, Mogil JS (2007) The Pain Genes Database: An interactive web browser of
860 pain-related transgenic knockout studies. Pain 131:3 e1-4.
861 Lacroix-Fralish ML, Austin JS, Zheng FY, Levitin DJ, Mogil JS (2011) Patterns of pain: meta-analysis of
862 microarray studies of pain. Pain 152:1888.
863 Laumet G, Garriga J, Chen SR, Zhang Y, Li DP, Smith TM, Dong Y, Jelinek J, Cesaroni M, Issa JP (2015)
864 G9a is essential for epigenetic silencing of K+ channel genes in acute-to-chronic pain
865 transition. Nature Neuroscience 18:1746-1755.
866 Lei L, Laub F, Lush M, Romero M, Zhou J, Luikart B, Klesse L, Ramirez F, Parada LF (2005) The zinc finger
867 transcription factor Klf7 is required for TrkA gene expression and development of nociceptive
868 sensory neurons. Gene Dev 19:1354-1364.
869 Li Z, Mao Y, Liang L, Wu S, Yuan J, Mo K, Cai W, Mao Q, Cao J, Bekker A, Zhang W, Tao Y-X (2017a) The
870 transcription factor C/EBPβ in the dorsal root ganglion contributes to peripheral nerve
871 trauma–induced nociceptive hypersensitivity. Science Signaling 10.
872 Li Z et al. (2017b) Targeting human Mas-related G protein-coupled receptor X1 to inhibit persistent
873 pain. Proceedings of the National Academy of Sciences of the United States of America
874 114:E1996-E2005.
875 Lou S, Duan B, Vong L, Lowell BB, Ma Q (2013) Runx1 Controls Terminal Morphology and
876 Mechanosensitivity of VGLUT3-expressing C-Mechanoreceptors. Journal of Neuroscience the
877 Official Journal of the Society for Neuroscience 33:870.
878 Lyko F (2017) The DNA methyltransferase family: a versatile toolkit for epigenetic regulation. Nature
879 Reviews Genetics 19.

880 Mamet J, Klukinov M, Harris S, Manning DC, Xie S, Pascual C, Taylor BK, Donahue RR, Yeomans DC
881 (2017a) Intrathecal administration of AYX2 DNA decoy produces a long-term pain treatment
882 in rat models of chronic pain by inhibiting the KLF6, KLF9, and KLF15 transcription factors.
883 Mol Pain 13:1744806917727917.
884 Mamet J, Klukinov M, Harris S, Manning DC, Xie S, Pascual C, Taylor BK, Donahue RR, Yeomans DC
885 (2017b) [EXPRESS] Intrathecal administration of AYX2 DNA-decoy produces a long-term pain
886 treatment in rat models of chronic pain by inhibiting the KLF6, KLF9 and KLF15 transcription
887 factors. Mol Pain 13:1744806917727917.
888 Masseck OA, Spoida K, Dalkara D, Maejima T, Rubelowski JM, Wallhorn L, Deneris ES, Herlitze S (2014)
889 Vertebrate Cone Opsins Enable Sustained and Highly Sensitive Rapid Control of Gi/o Signaling
890 in Anxiety Circuitry. Neuron 81:1263-1273.
891 Masuda T, Iwamoto S, Yoshinaga R, Tozakisaitoh H, Nishiyama A, Mak TW, Tamura T, Tsuda M, Inoue K
892 (2014) Transcription factor IRF5 drives P2X4R+-reactive microglia gating neuropathic pain.
893 Nature Communications 5:3771.
894 Moore DL, Apara A, Goldberg JL (2011) Kruppel-Like Transcription Factors in the Nervous System:
895 Novel players in neurite outgrowth and axon regeneration. Molecular & Cellular
896 Neuroscience 47:233.
897 Moore DL, Blackmore MG, Hu Y, Kaestner KH, Bixby JL, Lemmon VP, Goldberg JL (2009) KLF family
898 members regulate intrinsic axon regeneration ability. Science 326:298-301.
899 Nicol LS, Dawes JM, La Russa F, Didangelos A, Clark AK, Gentry C, Grist J, Davies JB, Malcangio M,
900 McMahon SB (2015) The Role of G-Protein Receptor 84 in Experimental Neuropathic Pain.
901 The Journal of neuroscience : the official journal of the Society for Neuroscience
902 35:8959-8969.
903 Niederberger E, Resch E, Parnham MJ, Geisslinger G (2017) Drugging the pain epigenome. Nature
904 Reviews Neurology 13:434-447.
905 Poetsch AR, Plass C (2011) Transcriptional regulation by DNA methylation. Cancer Treat Rev 37:S8-S12.
906 Pollemamays SL, Centeno MV, Apkarian AV, Martina M (2014) Expression of DNA methyltransferases in
907 adult dorsal root ganglia is cell-type specific and up regulated in a rodent model of
908 neuropathic pain. Frontiers in Cellular Neuroscience 8:217-217.
909 Qi L, Huang C, Wu X, Tao Y, Yan J, Shi T, Cao C, Han L, Qiu M, Ma Q, Liu Z, Liu Y (2017) Hierarchical
910 Specification of Pruriceptors by Runt-Domain Transcription Factor Runx1. The Journal of
911 Neuroscience 37:5549-5561.
912 Reinhold AK, Batti L, Bilbao D, Buness A, Rittner HL, Heppenstall PA (2015) Differential transcriptional
913 profiling of damaged and intact adjacent dorsal root ganglia neurons in neuropathic pain.
914 PloS one 10:e0123342.
915 Wolf L (2013) Opioid Receptors Revealed. Nature 90:383-383.
916 Xie RG, Gao YJ, Park CK, Lu N, Luo C, Wang WT, Wu SX, Ji RR (2017) Spinal CCL2 Promotes Central
917 Sensitization, Long-Term Potentiation, and Inflammatory Pain via CCR2: Further Insights into
918 Molecular, Synaptic, and Cellular Mechanisms. Neuroscience Bulletin:1-9.
919 Yanagi M, Hashimoto T, Kitamura N, Fukutake M, Komure O, Nishiguchi N, Kawamata T, Maeda K,
920 Shirakawa O (2008) Expression of Kruppel-like factor 5 gene in human brain and association
921 of the gene with the susceptibility to schizophrenia. Schizophrenia Research 100:291.
922 Yin K, Deuis JR, Lewis RJ, Vetter I (2016) Transcriptomic and behavioural characterisation of a mouse
923 model of burn pain identify the cholecystokinin 2 receptor as an analgesic target. Mol Pain

12.

Yu B, Zhang K, Milner JJ, Toma C, Chen R, Scott-Browne JP, Pereira RM, Crotty S, Chang JT, Pipkin ME (2017) Epigenetic landscapes reveal transcription factors that regulate CD8(+) T cell differentiation. Nature Immunology 18:573.

Zeilhofer HU, Wildner H, Yévenes GE (2012) Fast synaptic inhibition in spinal sensory processing and pain control. Physiological Reviews 92:193-235.

Zhang HH, Hu J, Zhou YL, Qin X, Song ZY, Yang PP, Hu S, Jiang X, Xu GY (2015) Promoted Interaction of Nuclear Factor-κB With Demethylated Purinergic P2X3 Receptor Gene Contributes to Neuropathic Pain in Rats With Diabetes. Diabetes 64:4272-4284.

Zhang Z, Cai YQ, Zou F, Bie B, Pan ZZ (2011a) Epigenetic suppression of GAD65 expression mediates persistent pain. Nat Med 17:1448-1455.

Zhao JY, Liang L, Gu X, Li Z, Wu S, Sun L, Atianjoh FE, Feng J, Mo K, Jia S (2017) DNA methyltransferase DNMT3a contributes to neuropathic pain by repressing Kcna2 in primary afferent neurons. Nature Communications 8:14712.

Zhou YL, Jiang GQ, Wei J, Zhang HH, Chen W, Zhu H, Hu S, Jiang X, Xu GY (2015) Enhanced binding capability of nuclear factor-κB with demethylated P2X3 receptor gene contributes to cancer pain in rats. Pain 156:1892.

Zhuang Z-Y, Gerner P, Woolf CJ, Ji R-R (2005) ERK is sequentially activated in neurons, microglia, and astrocytes by spinal nerve ligation and contributes to mechanical allodynia in this neuropathic pain model. Pain 114:149-159.

Zhuang ZY, Wen YR, Zhang DR, Borsello T, Bonny C, Strichartz GR, Decosterd I, Ji RR (2006) A peptide c-Jun N-terminal kinase (JNK) inhibitor blocks mechanical allodynia after spinal nerve ligation: respective roles of JNK activation in primary sensory neurons and spinal astrocytes for neuropathic pain development and maintenance. Journal of Neuroscience the Official Journal of the Society for Neuroscience 26:3551.

Figure legends

Figure 1. Generation of TALEN-mediated *GPR151* mutant mice. (A) A schematic shows the binding sites of TALENs (yellow) and space region (green) on Exon 1 of *GPR151*. FokI, an endonuclease. DSB, double-strand break; NHEJ, non-homologous end joining. (B) DNA sequencing shows the deletion of 7 bases (ATGGCCG) in the chimera mice (F0 generation).

Figure 2. GPR151 expression is increased in the spinal cord after SNL. (A) Gene chip shows the upregulation of several GPCRs genes after SNL. (B) There are 8 GPCRs whose expression was increased more than 1.5-fold after SNL. (C) The time course of *GPR151* mRNA expression in the ipsilateral dorsal horn in naïve, sham- and SNL-operated mice. * $p < 0.05$, ** $p < 0.01$, *** $p < 0.001$, vs. sham. Student's *t*-test. n=6 mice/group. SC, spinal cord. (D, E) In situ hybridization of *GPR151* mRNA shows that no signal was found in spinal sections incubated with *GPR151* sense probe (D), and positive signals were shown in spinal sections incubated with *GPR151* antisense probe (E). (F-H) In situ hybridization of *GPR151* mRNA and immunofluorescence staining with NeuN (F), GFAP (G) and IBA-1 (H). (I) Single-cell PCR shows the co-expression of *GPR151* with neuronal marker *NeuN*. (J, K) In situ hybridization of *GPR151* mRNA on the spinal cord from *SST*-GFP (J) and *GAD67*-GFP (K) mice 10 days after SNL. (L) The time course of *GPR151* mRNA expression in L5 DRG. ** $p < 0.01$, *** $p < 0.001$, vs. sham. Student's *t*-test. n=4-6 mice/group. (M-O) The images of in situ hybridization of *GPR151* mRNA in DRG sections incubated with *GPR151* sense probe (M) or *GPR151* antisense probe from naïve (N) or SNL (O) animals.

Figure 3. *GPR151* KO mice are normal in the expression of cellular markers and neurochemical markers. (A) PCR-based genotyping of WT and *GPR151*$^{-/-}$ mice. $^{+/+}$, $^{+/-}$ and $^{-/-}$ indicate WT, heterozygote, and homozygote. (B) Photographs of WT and *GPR151*$^{-/-}$ mice show no changes in the gross anatomy of the *GPR151*$^{-/-}$ mice. (C) *GPR151*$^{-/-}$ mice show normal distribution patterns in the spinal dorsal horn of the neurochemical marker NeuN, astrocytic marker GFAP, and microglial marker Iba-1. (D) The expression of IB4^{+} non-peptidergic primary afferents, CGRP^{+} peptidergic primary afferents, and neurochemical marker PKCγ is normal in *GPR151*$^{-/-}$ mice.

Figure 4. Mutation or inhibition of GPR151 alleviates SNL-induced neuropathic pain. (A) Acute pain threshold measured by tail immersion, Hargreaves test, von Frey test and motor function assessed by the Rota-rod test were comparable in WT and *GPR151*$^{-/-}$ mice. n=8-9 mice/group. Student's *t*-test. (B, C) SNL-induced mechanical allodynia (B) and heat hyperalgesia (C) were markedly alleviated in *GPR151*$^{-/-}$ mice compared with WT mice. n= 6-7 mice/group. * $p < 0.05$, ** $p < 0.01$, *** $p < 0.001$, vs. WT. Two-way RM ANOVA followed by Bonferroni's tests. (D, E) Intraspinal infusion of LV-*GPR151* shRNA in the spinal cord alleviated SNL-induced mechanical allodynia 7 days after SNL (D) and blocked heat hyperalgesia (E). * $p < 0.05$, ** $p < 0.01$, *** $p < 0.001$, vs. LV-NC. Two-way RM ANOVA followed by Bonferroni's tests. n=5-6 mice/group.

Figure 5. Demethylation of *GPR151* gene promoter region after SNL. (A) The schematic shows the location of 10 CpG sites (red) within a CpG island of the *GPR151* gene promoter region. (B) Representative PCR shows that the ratio of methylated (M) to unmethylated (U) amplification

products was reduced after SNL. * $p < 0.05$, vs. sham. Student's *t*-test. n=4 mice/group. (C) Bisulfite sequencing of *GPR151* promoter region of the spinal dorsal horn in sham- or SNL-operated mice. n=3 mice/group. Ten clones were randomly selected from each mouse. Filled circles, methylated CpG sites. Unfilled circles, unmethylated CpG sites. (D) The total methylation of GPR151 promoter was decreased after SNL. * $p < 0.05$, SNL vs. sham. Two-way RM ANOVA followed by Bonferroni's tests. n=3 mice/group. (E) Coelenterazine-utilizing luciferase assay shows that the luciferase activity was increased when using HEK-293 cells transfected with the unmethylated pCpG-free-*GPR151*-promoter-Lucia vector. *** $p < 0.001$. Student's *t*-test. n=4 /group. (F) Western blot shows that DNMT3b protein level was decreased after SNL. *** $P < 0.001$, vs. naïve. n=3 mice/group. (G) ChIP-PCR shows that the binding of DNMT3b with *GPR151* in the spinal dorsal horn was decreased after SNL. * $p < 0.05$, Student's *t*-test. n=5 mice/group. (H) The mRNA expression of *DNMT3b* was decreased and *GPR151* was increased 2 days after intrathecal injection of *DNMT3b* siRNA. ** $p < 0.05$, vs. NC. Student's *t*-test. n=6-7 mice/group. (I) The ratio of methylated to unmethylated products of *GPR151* promoter was decreased after intrathecal injection of *DNMT3b* siRNA. * $P < 0.05$, vs. NC. Student's *t*-test. n=4 mice/group. (J) Intrathecal injection of *DNMT3b* siRNA induced mechanical allodynia. * $p < 0.05$, ** $p < 0.01$, vs. NC. Two-way RM ANOVA followed by Bonferroni's tests. n=7-8 mice/group. (K) The mRNA expression of *DNMT3b* was increased and *GPR151* was decreased after intraspinal infusion of LV-*DNMT3b*. *** $p < 0.001$, vs. LV-NC. Student's *t*-test. n=6-7 mice/group. (L) Pretreatment with LV-*DNMT3b* increased the methylation of *GPR151* promoter in the spinal dorsal horn 10 days after SNL. * $p < 0.05$, vs. LV-NC. Student's *t*-test. n=4 mice/group. (M) Intraspinal infusion of LV-*DNMT3b*, 3 days before SNL, alleviated SNL-induced mechanical

allodynia. *$p < 0.05$, ** $p < 0.01$, vs. LV-NC. Two-way RM ANOVA followed by Bonferroni's tests. n=6-7 mice/group.

Figure 6. The transcription factor KLF5 promotes the expression of GPR151. (A) Schematic representation of *GPR151* promoter region. Putative binding sites for KLF5, STAT3, and NFATC2 transcription factors are shown. (B) The schematic shows the location of potential binding sites (red) of KLF5 with the *GPR151* promoter region within the CpG sites. (C) The logos of the standard *KLF5* motif and 5 potential binding sites of KLF5 with *GPR151* promoter (BS1-5). (D) ChIP–PCR shows that the binding of KLF5 with *GPR151* was increased after SNL. * $p < 0.05$, vs. sham. Student's *t*-test. n=4 mice/group. (E) Coelenterazine-utilizing luciferase assay shows that the luciferase activity was dramatically increased when KLF5-expressing vector was transfected with unmethylated pCpG-free-*GPR151*-promoter-Lucia vector in HEK293 cells. *** $p < 0.001$. Student's *t*-test. n=4 /group. (F) The luciferase reporter assay shows that the luciferase activity was decreased when co-transfection of KLF5-expressing vector with mutant KLF5 binding site 3 (BS3) or 4 (BS4) (right). *** $p < 0.001$, vs. Basic vector. ### $p < 0.001$, vs. *GPR151* vector. One-way ANOVA. n=4 /group.

Figure 7. KLF5 is increased in the spinal cord after SNL and contributes to SNL-induced neuropathic pain. (A) The time course of *KLF5* mRNA expression in the spinal cord from naïve and SNL-operated mice. The mRNA expression of *KLF5* was increased at days 1, 3, 10, and 21 after SNL. * $p < 0.05$, *** $p < 0.001$, SNL vs. naïve. One-way ANOVA. n=5-6 mice/group. (B-C) Representative images of KLF5 immunofluorescence in the spinal cord from naïve and SNL mice.

KLF5 was constitutively expressed in naïve mice (B), and increased in SNL-operated mice (C). (D-F) Double immunofluorescence staining shows that KLF5 was mainly colocalized with the neuronal marker NeuN (D), a few with astrocyte marker GFAP (E), none with microglia marker CD11b (F) in the dorsal horn of spinal cord 10 days after SNL. (G) In situ hybridization of *GPR151* and immunostaining with KLF5 in the spinal cord 10 days after SNL. (H, I) Immunostaining of KLF5 on the spinal cord from *SST*-GFP (H) and *GAD67*-GFP (I) mice 10 days after SNL. Arrows show typical double-staining neurons. Filled triangles show typical KLF5-single labeled neurons. Blank triangles show SST- (in H) or GAD67-single labeled (in I) neurons. (J, K) Intrathecal injection of *KLF5* siRNA alleviated SNL-induced mechanical allodynia (J) and heat hyperalgesia (K). * $p < 0.05$, vs. NC siRNA. Two-way RM ANOVA followed by Bonferroni's tests. n=6-7 mice/group. (L) The mRNA expression of *KLF5* and *GPR151* were decreased after intrathecal injection of *KLF5* siRNA. * $p < 0.05$, ** $p < 0.01$, vs. NC siRNA. Student's *t*-test. n=6-8 mice/group. (M-N) Intrathecal injection of KLF5 inhibitor, ML264, 10 days after SNL alleviated SNL-induced mechanical allodynia (M) and thermal hyperalgesia (N). *** $p < 0.001$, vs. Vehicle. Two-way RM ANOVA followed by Bonferroni's tests. n=5-9 mice/group. (O) The mRNA expression of *KLF5* and *GPR151* was decreased after intrathecal injection of ML264. * $p < 0.05$, vs. vehicle, Student's *t*-test. n=7-9 mice/group.

Figure 8. Gene expression profiles in the spinal cord of WT and *GPR151* deficient mice after SNL. (A) A scatter plot shows the gene expression in WT and *GPR151*$^{-/-}$ mice. Red dots represent upregulated genes, and green dots represent downregulated genes. (B) Heat map of expression of differentially expressed genes whose expression changes were more than 2-fold in SNL group,

compared with the sham group. A dendrogram (top) shows the clustering of the samples regarding these expression values (n=2/group). (C) Heat map representing expression values of 41 pain-related genes from Pain Gene database that were up-regulated by nerve injury and normalized to the sham control after *GPR151* mutation. (D) Heat map representing expression values of 39 pain-related genes from Pain Gene database that were up-regulated in SNL *GPR151*$^{-/-}$ group, comparing with the WT-SNL group. (E) The significant pathways for down-regulated genes in *GPR151*$^{-/-}$-SNL group. The MAPK pathway-associated genes were down-regulated dramatically in *GPR151*$^{-/-}$-SNL mice compared to WT-SNL mice. (F) The significant pathways for up-regulated genes in *GPR151* mutation group. (G) RT-PCR for *FGF14, PRKACA, CRK, MAP3K13,* and *GRB2* gene expression levels in WT and *GPR151*$^{-/-}$ mice 10 days after SNL. ** $p < 0.01$. Student's *t*-test, n=4 mice/group. (H, I) Western blots for pERK, pp38, and pJNK in the spinal cord from WT and *GPR151*$^{-/-}$ mice 10 days after sham or SNL operation. * $p < 0.05$, Student's *t*-test, n=3 mice/group.

Figure 9. Schematic shows the epigenetic regulation of GPR151 expression and the mechanism of GPR151 underlying neuropathic pain. (A) In healthy spinal cord, DNMT3b binds to the *GPR151* promoter and silences its expression through DNA methylation. (B) After nerve injury, DNMT3b dissociates from the *GPR151* gene promoter following by active DNA demethylation, which induces chromatin accessibility, thereby promotes the recruitment of the transcriptional machinery. The transcription factor KLF5 is recruited onto the GPR151 gene promoter, facilitates GPR151 transcription, and further increases the expression of GPR151 protein. The increased GPR151 on the membrane is activated by extracellular signals and induce

1091 the action of ERK. The pERK translocates into the nucleus and induces the expression of multiple
1092 algogenic genes that participate in pain processing, leading to the pathogenesis of neuropathic
1093 pain.
1094

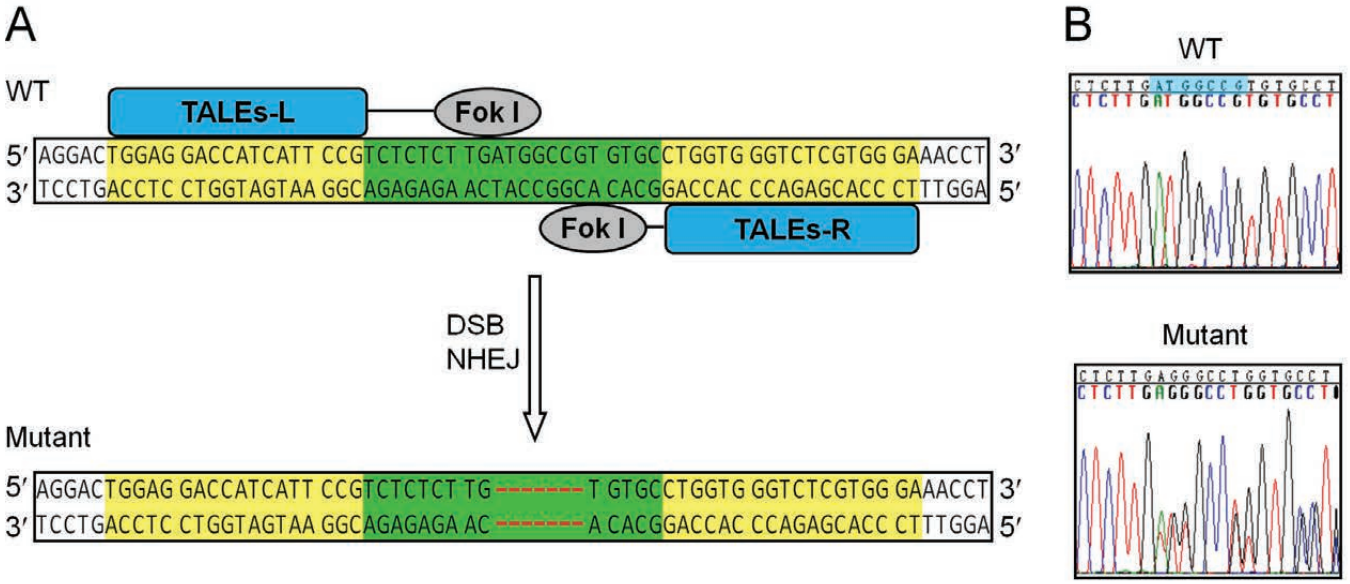

A

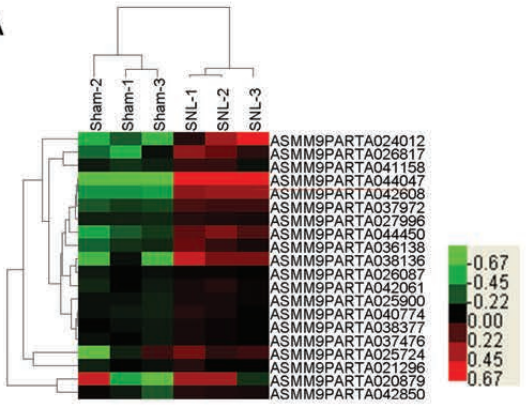

B

Fold of change	Gene symbol	Probe ID
26.294	*GPR151*	ASMM9PARTA044047
5.218	*GPR150*	ASMM9PARTA042608
3.006	*GPR84*	ASMM9PARTA037972
2.358	*GPR160*	ASMM9PARTA024012
1.947	*GPR124*	ASMM9PARTA038136
1.774	*GPR152*	ASMM9PARTA044450
1.713	*GPR174*	ASMM9PARTA026817
1.530	*GPR160*	ASMM9PARTA036138

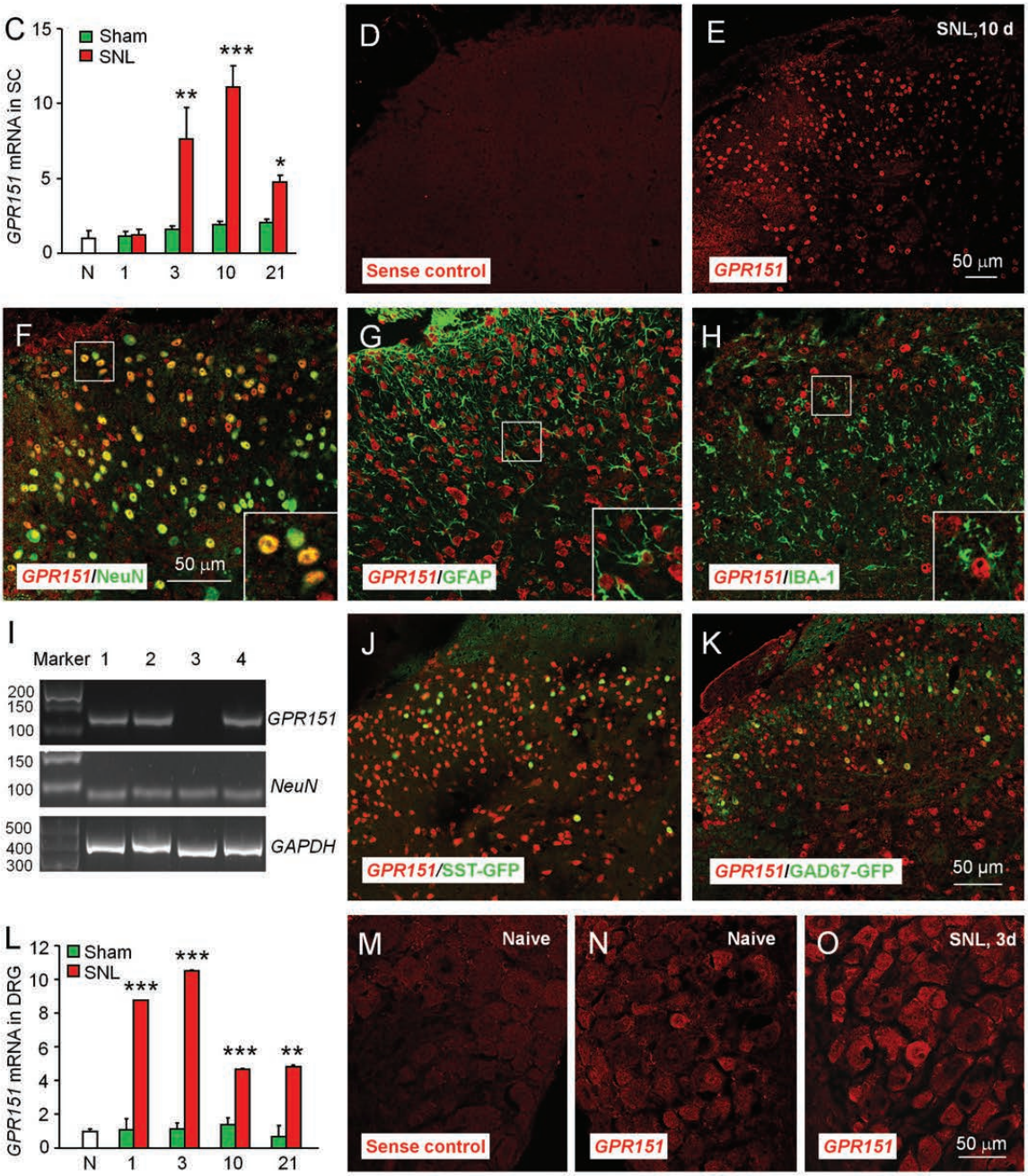

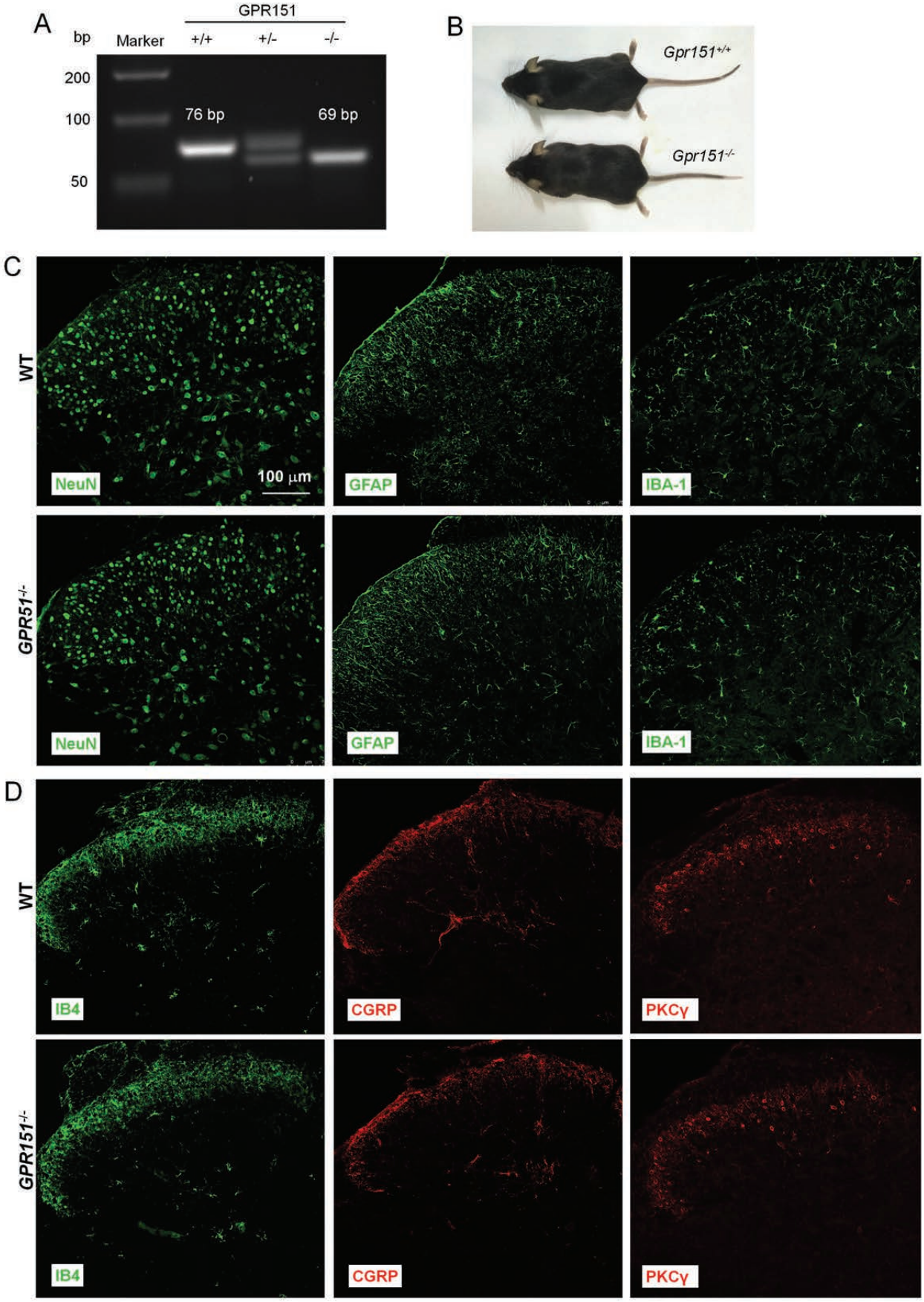

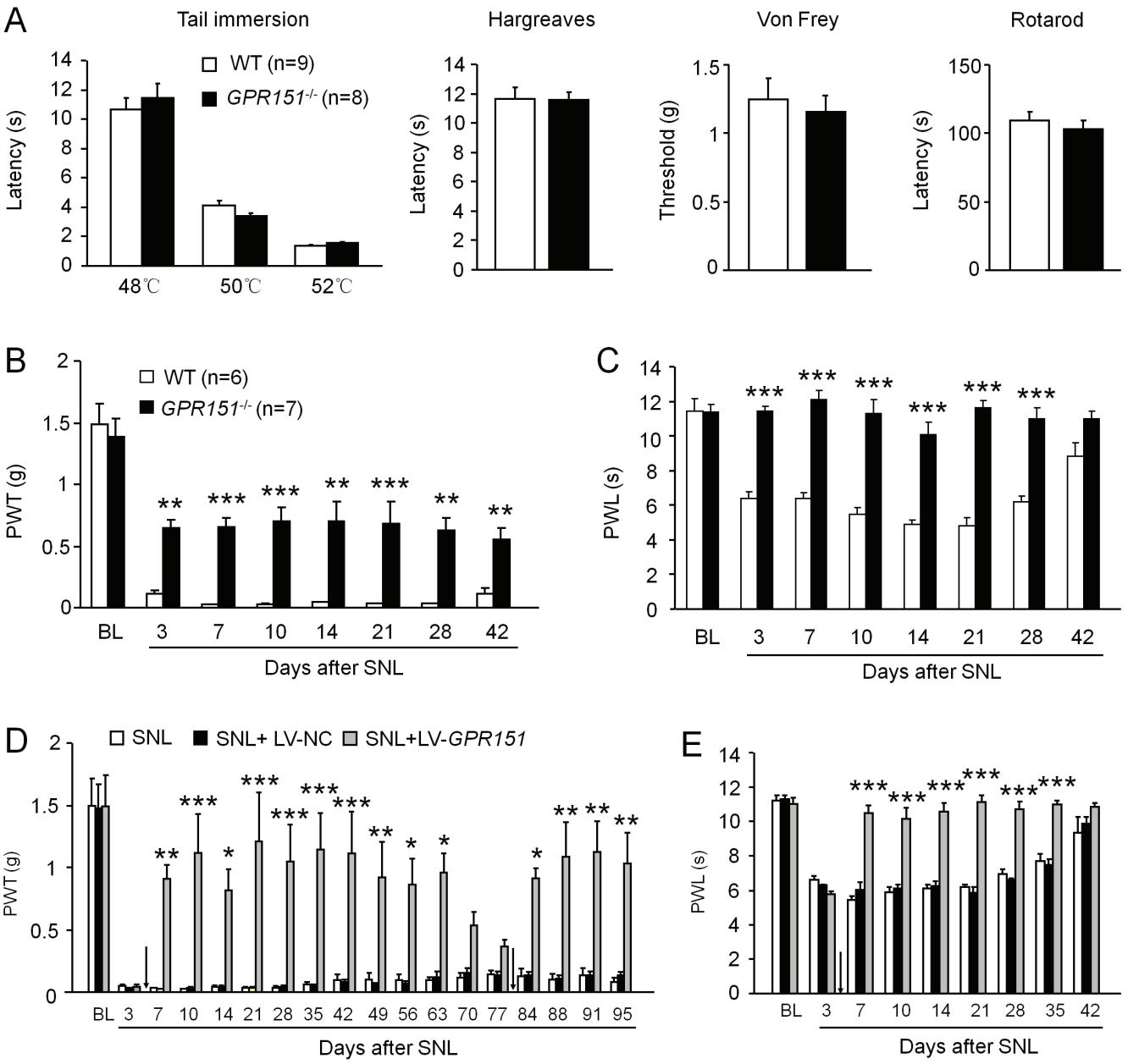

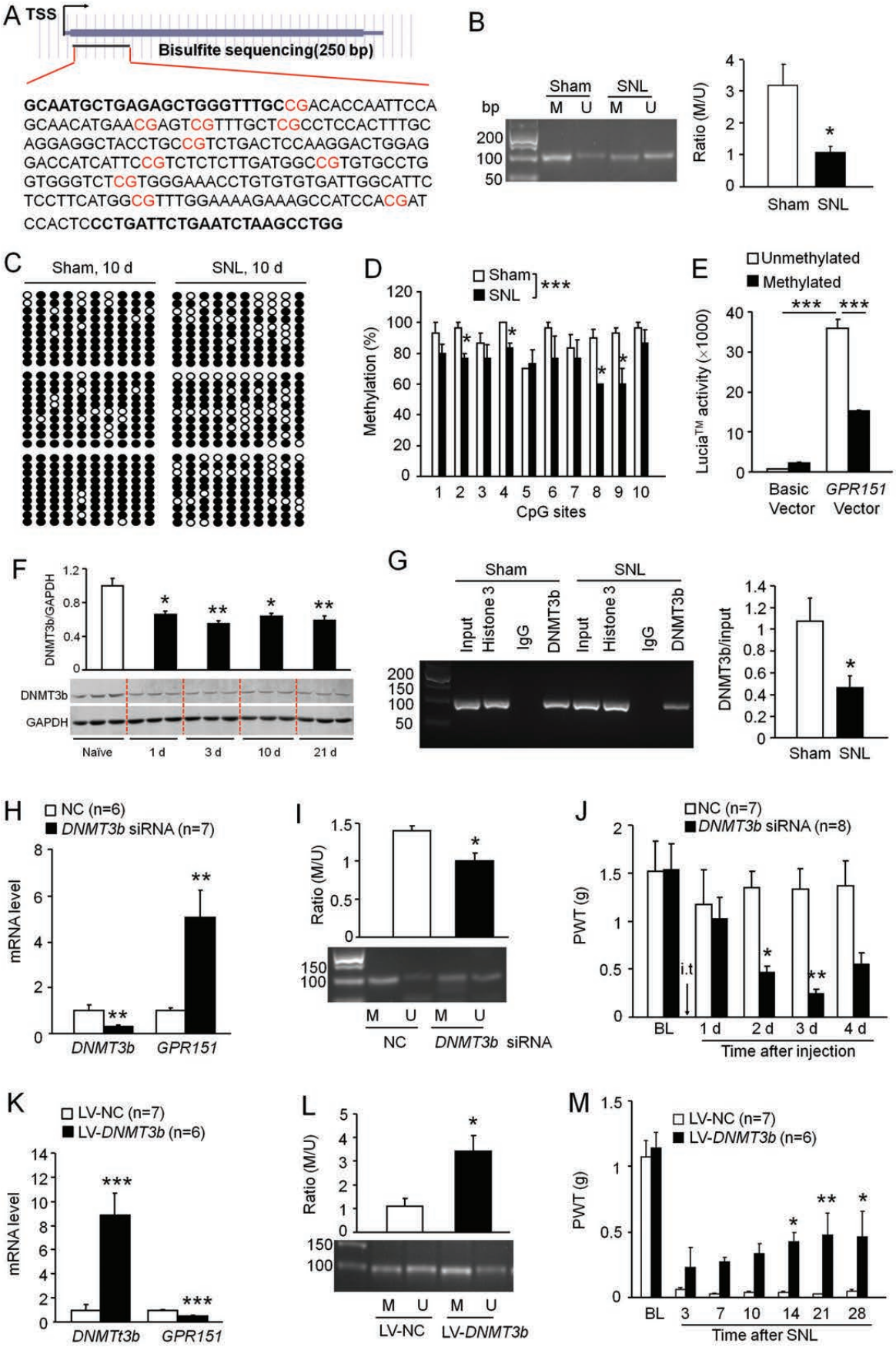

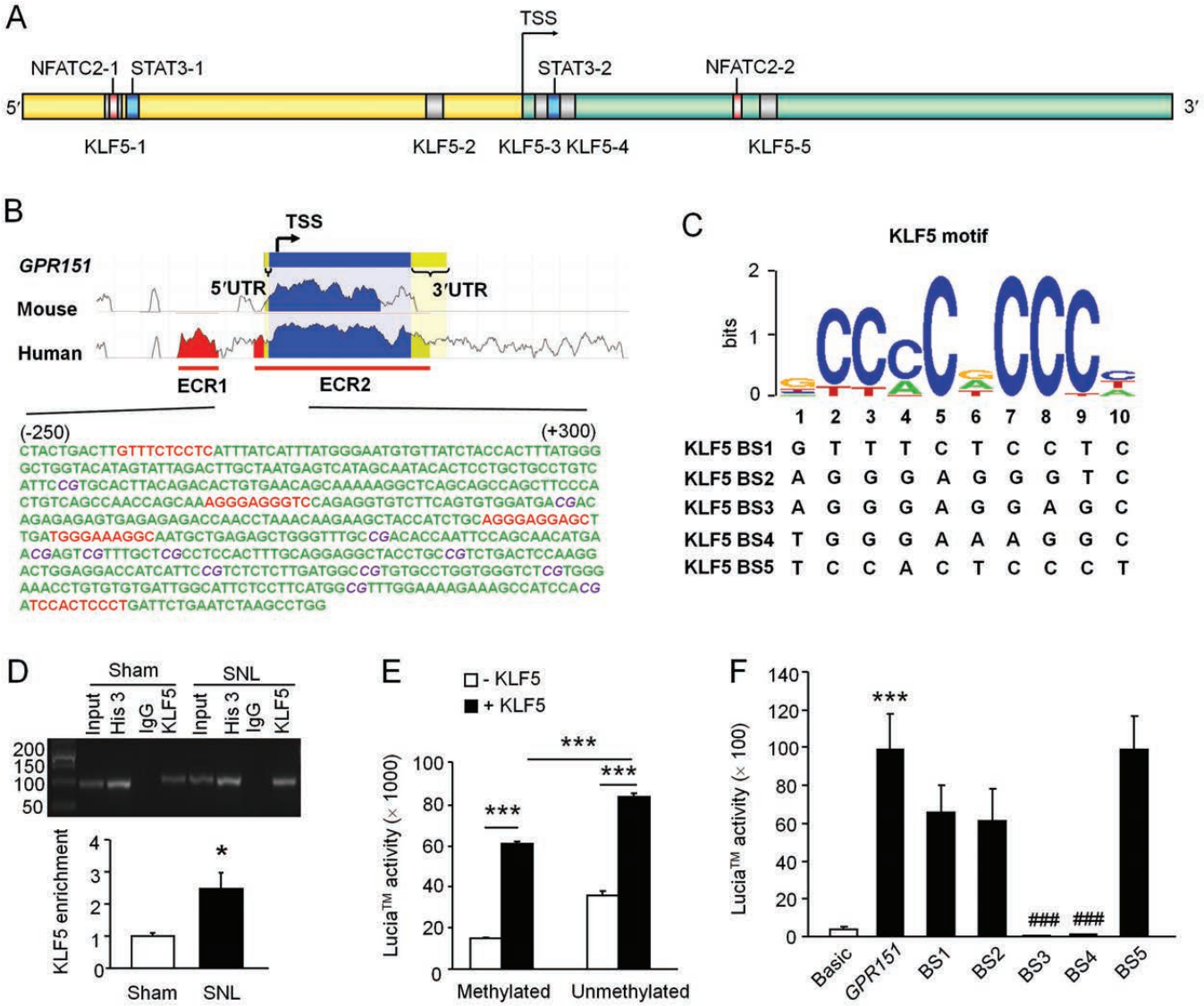

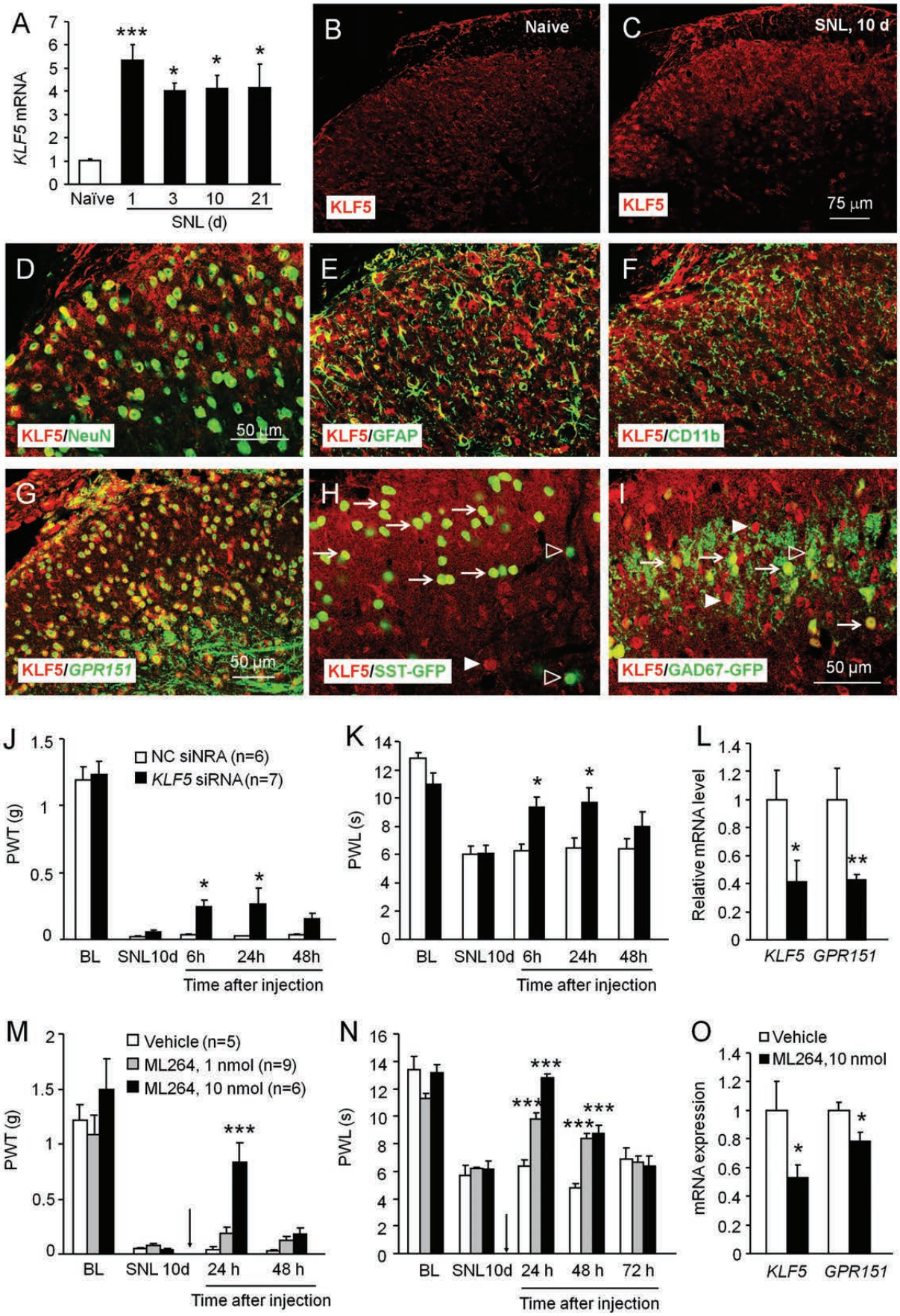

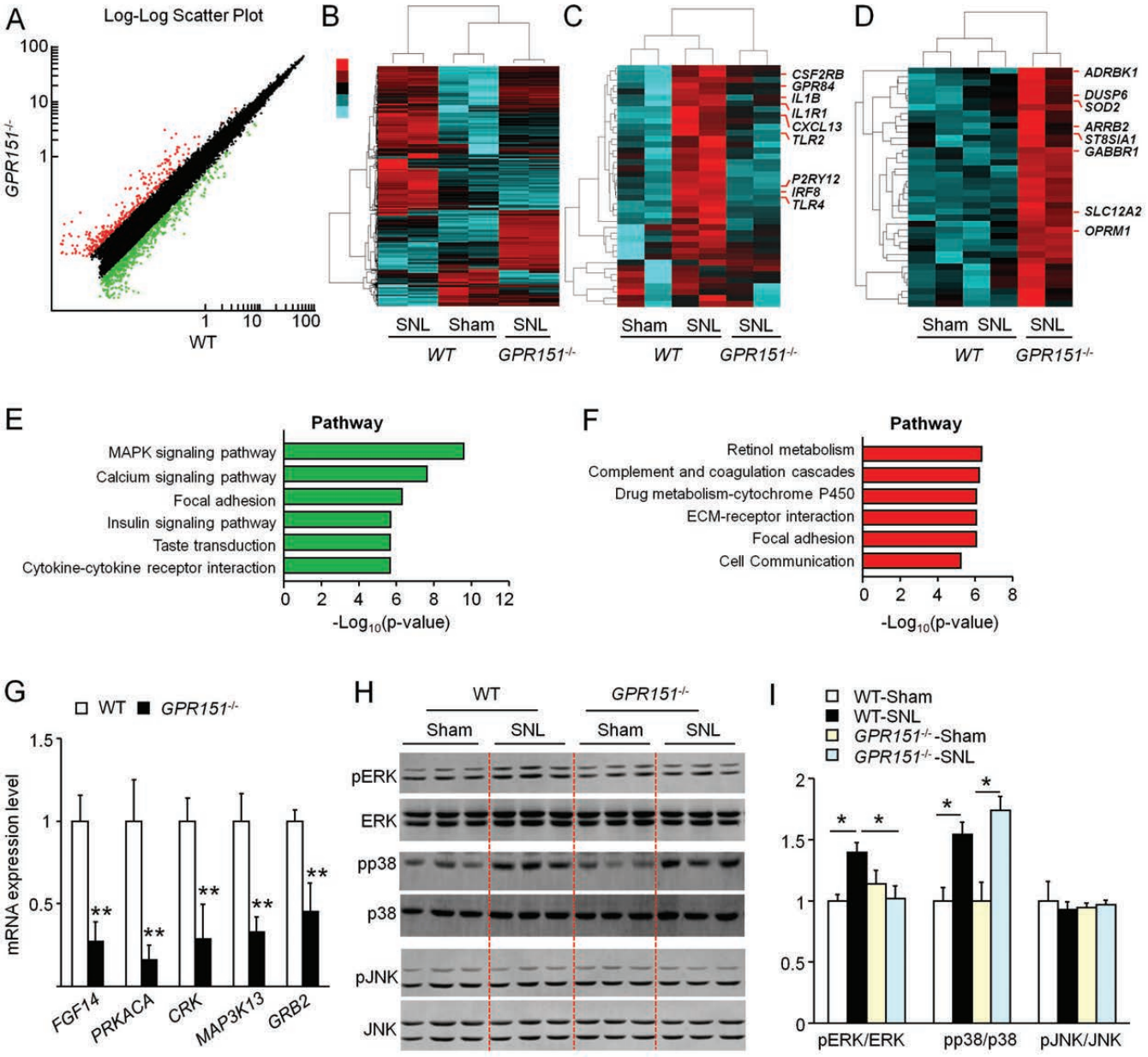

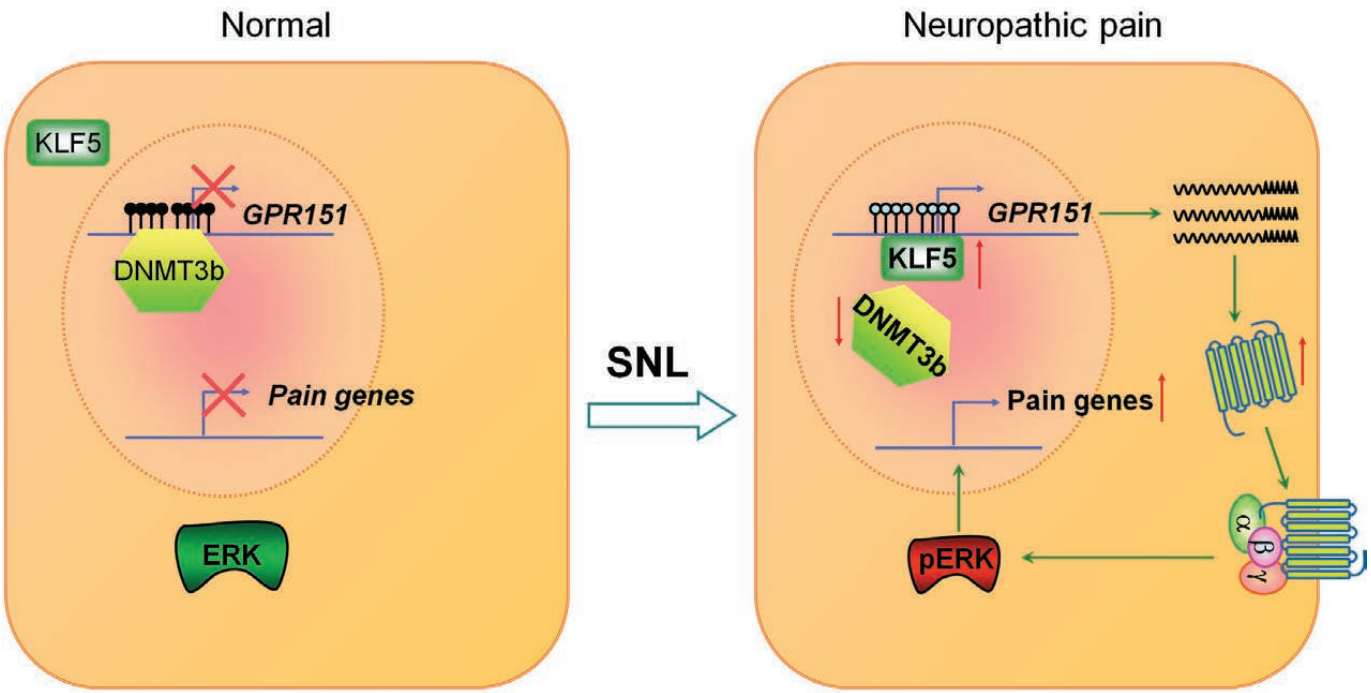

Table 1. Primers sequences for Real-time PCR

Gene	Primers	Primer Sequence (5′-3′)	Amplicon size
GAPDH	Forward	GCTTGAAGGTGTTGCCCTCAG	201 bp
	Reverse	AGAAGCCAGCGTTCACCAGAC	
GPR151	Forward	ACACGAAGGCCAAGAGACAG	273 bp
	Reverse	GCCAGCGTGAGCCCTATAAT	
DNMT3b	Forward	CTGTCCGAACCCGACATAGC	120 bp
	Reverse	CCGGAAACTCCACAGGGTA	
KLF5	Forward	CCGGAGACGATCTGAAACACG	233 bp
	Reverse	GTTGATGCTGTAAGGTATGCCT	
FGF14	Forward	TTCTCAGGGTGTCTAAGCTGC	141 bp
	Reverse	GGGGATCAGTTGGGTTCTTGTT	
PRKACA	Forward	AGATCGTCCTGACCTTTGAGT	119 bp
	Reverse	GGCAAAACCGAAGTCTGTCAC	
CRK	Forward	GGAGGTCGGTGAGCTGGTA	75 bp
	Reverse	CGTTTGCCATTACACTCCCCT	
MAP3K13	Forward	CCCGACCTCATCTCCACAG	113 bp
	Reverse	TGGAAACAGGGATCATAGGGTT	
GRB2	Forward	ACAGCTAGGCAGATTTCCAGG	124 bp
	Reverse	CAAGACAGCCCCAGTAGGT	

Table 2. Primers sequences for single-cell PCR.

Gene	Primers	Primer Sequence (5′-3′)	Amplicon size
GPR151-OUT	Forward	GGTTTGCCGACACCAATTCC	314 bp
	Reverse	GAACCAGCCGAGATCCCAAA	
GPR151-IN	Forward	GTTTGCTCGCCTCCACTTTG	119 bp
	Reverse	CACACAGGTTTCCCACGAGA	
NeuN-OUT	Forward	AGACAGACAACCAGCAACTC	357 bp
	Reverse	CTGTTCCTACCACAGGGTTTAG	
NeuN-IN	Forward	ACGATCGTAGAGGGACGGAA	86 bp
	Reverse	TTGGCATATGGGTTCCCAGG	
GAPDH-OUT	Forward	AGCCTCGTCCCGTAGACAAAA	367 bp
	Reverse	TTTTGGCTCCACCCCTTCA	
GAPDH-IN	Forward	TGAAGGTCGGTGTGAACGAATT	313 bp
	Reverse	GCTTTCTCCATGGTGGTGAAGA	

Table 3. Primers sequences for BSP, MSP and ChIP experiment.

Gene	Primers	Primer Sequence (5′-3′)	Amplicon size
*GPR151*MSP	Forward	ATATGAATGAGTCGTTTGTTC	100 bp
Unmethylated	Reverse	ACACAACCATCAAAAAAAACG	
*GPR151*MSP	Forward	GTAATATGAATGAGTTGTTTGTTT	100 bp
Methylated	Reverse	ACACAACCATCAAAAAAAACAA	
*GPR151*BSP	Forward	GTAATGTTGAGAGTTGGGTTTGT	250 bp
	Reverse	CCAAACTTAAATTCAAAATCAAA	
GPR151 ChIP	Forward	GTTTGCTCGCCTCCACTTTG	119 bp
	Reverse	CACACAGGTTTCCCACGAGA	